

**ILLINOIS INSTITUTE
OF TECHNOLOGY**



2023 DESIGN BUILD FLY REPORT

ILLINOIS INSTITUTE OF TECHNOLOGY
2023 AIAA-DBF DESIGN REPORT

Contents

1 Executive Summary	5
2 Management Summary	6
2.1 Milestone Chart	7
2.2 Budget	8
3 Conceptual Design	9
3.1 Mission Requirements	9
3.2 Design Requirements	11
3.3 Score Sensitivity	12
3.4 Configuration Selection	13
3.5 Propulsion Sizing	16
3.6 Wing and Jamming Antenna Integration	17
3.7 Final Results	17
4 Preliminary Design	17
4.1 Description of Design Methodology	17
4.2 Box Sizing Trade	19
4.3 Preliminary Aircraft Sizing	20
4.4 Aerodynamics Airfoils, Lift, Drag	21
4.5 Aircraft Stability	23
4.6 Estimated Aircraft Mission Performance	27
5 Detail Design	28
5.1 Structures Final Dimensional Parameters	28
5.2 Wing Design	28
5.3 Antenna Design	30
5.4 Tail Design	30
5.5 Fuselage Design	31
5.6 Landing Gear	33
5.7 Box Design	34
5.8 Payload	34
5.9 Weight and Balance	35
5.10Final 3D Render	36
5.11 Drawing Package	36

6 Manufacturing Plan	41
6.1 Manufacturing Plan	41
6.2 Methods Considered	41
6.3 Materials Considered	42
6.4 Subsystem Manufacturing	42
6.5 Landing Gear	45
6.6 Manufacturing Milestone Chart	46
7 Testing Plan	47
7.1 Testing Milestone Chart	47
7.2 Structural Test	47
7.3 Motor Test	48
7.4 Wing Tip Test	48
7.5 Flight Test	49
7.6 Flight Test Check List	49
8 Performance Results	51
8.1 Structural Endurance Results	51
8.2 Propulsion Results	51
8.3 Wing Tip Test Result	52
8.4 Flight Test Result	52
8.5 Comparison of Prediction vs. Actual	54
References	56

Abbreviations

α	Aircraft angle of attack [deg]	RC	Remote-Controlled
ρ	Air density [slug/in. ³]	Re	Reynold's number
AIAA	American Institute of Aeronautics & Astronautics		
ω_d	Damped frequency [rad/s, Hz]	S	Wing area [in. ² , ft. ²]
ω_n	Natural frequency [rad/s, Hz]	S_{wet}	Wetted area
ζ	Damping ratio [-]	AR	Aspect ratio [-]
TE	Trailing Edge		
b	Wingspan [in, ft]	θ	Theta
c	Wing chord [in]	T/W	Thrust-to-weight ratio [-]
C_d, C_D	Drag coefficient (2D, 3D) [-]	UAV	Unmanned aerial vehicle
C_{D0}	Zero-lift drag coefficient	W/S	Wing loading [-]
C_f	Skin friction coefficient	v	Velocity [ft/s]
C_{HT}	Horizontal tail coefficient [-]	Wh	Watt-hours
C_l, C_L	Lift coefficient (2D, 3D) [-]		
$C_{L_{max}}$	Maximum lift coefficient [-]		
C_m, C_M	Moment coefficient (2D, 3D) [-]		
C_{VT}	Vertical tail coefficient [-]		
CA	Cyanoacrylate adhesive		
CAD	Computational Aided Design		
CFD	Computational fluid dynamics		
CG	Center of gravity [in]		
D	Drag		
DBF	Design, Build, Fly		
e	Oswald efficiency		
ESC	Electronic speed controller		
g	acceleration of gravity		
GM	Ground mission score		
IIT	Illinois Institute of Technology		
LE	Leading Edge		
LiPo	Lithium Polymer		
L	Lift		
L/D	Lift-to-drag ratio [-]		
mAH	milli-Amp Hours		
M_1	Mission 1 score		
M_2	Mission 2 score		
M_3	Mission 3 score		



1 Executive Summary

This report serves to outline the design, manufacturing, and testing processes of the Illinois Institute of Technology (IIT) 2022-23 DBF team. The team's objective is to design and manufacture an electronic warfare aircraft for various surveillance and signal jamming missions. DBF's mission requirements dictate that the aircraft must fit inside an airline checked shipping box with maximum total additive dimensions of 62 inches.

Mission requirements dictate that the aircraft must be able to fit within specified dimension of a box, where each length must sum to 62 inches in total length. The UAV must be capable of completing three missions and a ground mission as described in Section 3.1. Mission 1 requires three laps in five minutes with no payload. Mission 2 requires as many laps in ten minutes, while carrying the payload in its shipping container to simulate the electronics package. Mission 3 requires the affixing of the wingtip antenna and flying three laps as fast as possible. A ground mission will also evaluate the wing tip loading of the airplane.

Score analysis was conducted by applying numerical preferences in chronological order, with 0 being the lowest and 1 being the highest for Mission 1, and the numbers for the other missions dependent on the particular scoring method from the rules.

To maximize the overall score, the team first conducted sensitivity analyses based on the maximum electronic package weight that can be carried for Mission 2 and the length of the jamming antenna that can be accommodated for Mission 3. Additionally, the aircraft must complete all three missions and a ground mission as described in Table 3.1. The results of this analysis were incorporated into the team's preliminary design. An overview of the team's structure is shown in Section 2. Following this, Section 3 discusses the approach used to develop a design as well as the individual sub-teams' methods. A conventional single fuselage, high wing, monoplane with a conventional tail was selected during the early design stage due to its ease of manufacturing and payload capacity, which is further described in Section 4. The detail design plans are covered in Section 5. The aircraft will be constructed using various woods and MonoKote, as illustrated in the manufacturing layout found in Section 6. Finally, the aircraft will go through a testing regiment defined in Section 7 and results will be discussed in Section 8.

2 Management Summary

The team is student led and consists of three sub-teams, acting as separate entities for part of the design process. A faculty advisor was consulted for constructive criticism and an alternative perspective; he was chosen due to his experience building and flying Remote-Controlled (RC) planes, as well as significant full-scale aircraft design expertise. Students were organized into leads, a Chief Engineer, and Project Manager. A student with strengths in organization is the Project Manager. A student with the most experience and technical knowledge is the Chief Engineer. The Chief Engineer and Project Manager worked together throughout project development to ensure work was completed accurately and efficiently. All leadership roles are held by students with previous experience in DBF.

The Project Manager's primary responsibilities consist of keeping track of project progress, delegating tasks, overseeing communications, and providing assistance where needed. The Chief Engineer's primary responsibilities consist of providing specific design constraints, time projections per task, and requesting specific administrative assistance throughout project phases. Assignments were delegated to all members, regardless of experience or ranking, to encourage participation, and foster an educational experience for all team members. Three sub-teams, Aerodynamics, Propulsion, and Structures, are led by senior and junior students with expertise and experience in their respective fields. These branches provided a means for members to gain and apply knowledge on a particular area of the design.

The majority of tasks were done collaboratively with subteams handling specifics related to their branch. The hierarchy of the team is shown in Figure 2.1.

IIT's team is student run and has a faculty advisor present to provide necessary guidance. The team is composed of multiple sub-teams that are each responsible for a major design component of the aircraft. Table 2.1 describes the roles and skills utilized by each sub-team. A sub-team is led by a team lead who reports to the Project Manager and Chief Engineer. The Chief Engineer oversees all components of the design and ensures cohesion between all sub-team decisions. The Chief Engineer also reports progress and design decisions to the Project Manager. The Project Manager is responsible for ensuring the design progress stays on track, deadlines are being met, and team leads are focusing resources on appropriate tasks and functions.

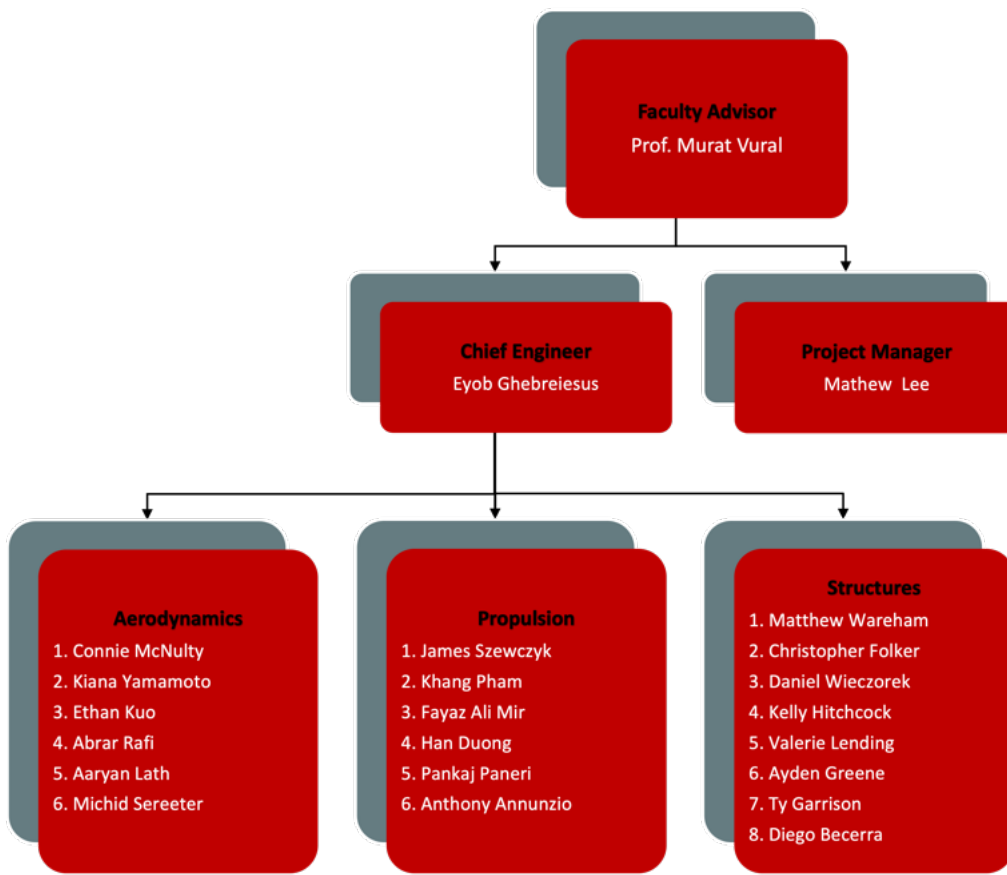


Figure 2.1 – Illinois Tech Team Organisation

Table 2.1 – Description and skills utilized and learned for each sub-team.

Sub-team	Responsibilities	Associated Skills
Aerodynamics	Design of lifting bodies, aircraft sizing, aerodynamic performance, and stability analysis.	<ul style="list-style-type: none">• Aerodynamics and flight mechanics• XFLR5 and related CFD software
Propulsion	Selection of motor/battery combination, setup of remote control systems, and flight data analysis.	<ul style="list-style-type: none">• Propulsion sizing tools• Electrical design• System analysis and feedback control
Structures	Design of aircraft structures, mechanical systems, and shipping container along with material selection.	<ul style="list-style-type: none">• Structural mechanics• CAD and FEA software

2.1 Milestone Chart

A Gantt chart, as shown in Figure 2.2, is maintained by the Project Manager to monitor project status and distribute resources accordingly. The schedule serves to keep track of the planned and actual schedules, due dates, delays, and appropriate task orders.

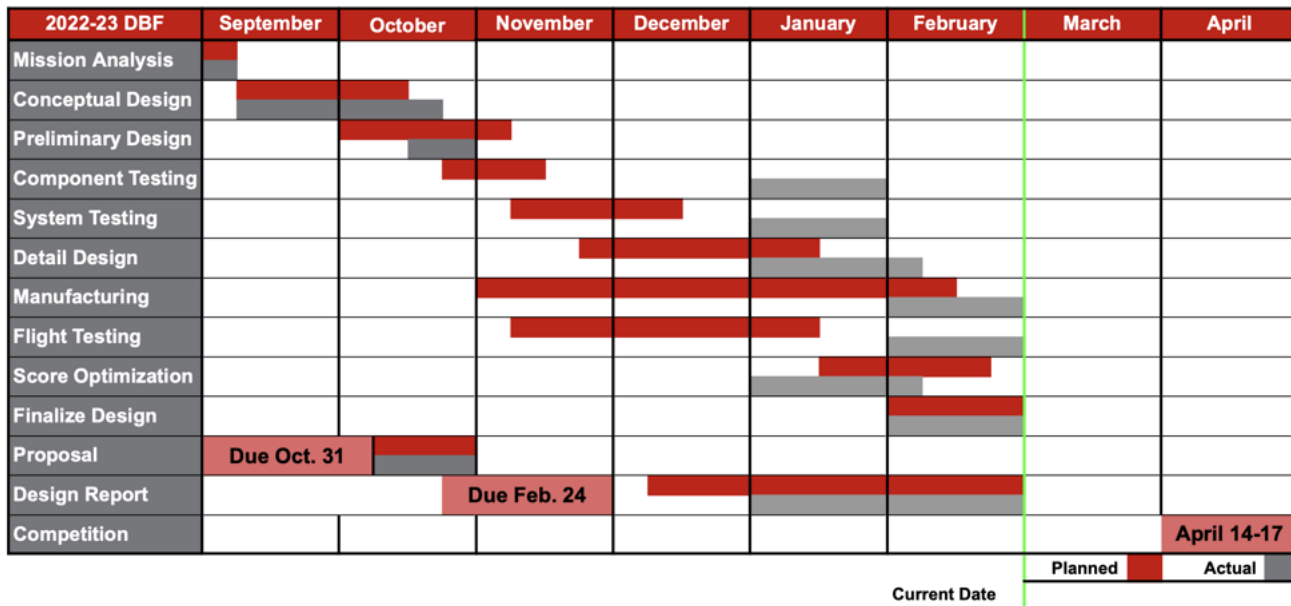


Figure 2.2 – Illinois Tech Team Milestone Chart

2.2 Budget

The project will be funded by the Illinois Institute of Technology Student Activity Fund (IIT-SAF). IIT-SAF will fund the entirety of materials and components for testing, design, and all of the costs associated with travel to the competition. A summary of the expected expenses are shown in Table 2.2. The necessary machines and tools are available in IIT's Idea Shop and the AIAA-IIT lab which has been furnished by IIT Student Activities Fund.

Table 2.2 – Proposed Budget with Funding Sources

Expenses	Description	Cost	Funding Source
Structural materials	Balsa, plywood, adhesives, hardware	\$1120	100% IIT-SAF
Propulsion System	Motors, ESC, battery, propeller	\$385	100% IIT-SAF
Control system	Wiring, servos, RC controller, receiver	\$130	100% IIT-SAF
Miscellaneous	Landing gear, MonoKote, tools	\$225	100% IIT-SAF
Air Travel	9 Students, \$450 per person	\$4050	100% IIT-SAF
Hotel	3 rooms for 4 nights	\$1800	100% IIT-SAF
Transportation	2 Cars for 5 days + gas	\$1500	100% IIT-SAF
Total		\$9210	

3 Conceptual Design

The conceptual design stage of the aircraft used contest scoring and design restrictions to optimize design parameters. These parameters were used to compare various aircraft configurations to select the highest scoring configuration. This section presents the final selected plane configuration, and its maximum weighted points.

3.1 Mission Requirements

AIAA's 2023 DBF rules specify that the plane must be designed with the capability to transport an electronic warfare package, and having a jamming antenna mounted on one of the wings. This jamming antenna is specified to 0.5 inch thickness with a payload box that has to have dimensions of at least 3 in x 3 in x 6 in. Additionally, the entire plane and its set components must be able to fit inside a shipping box with its total sum of linear dimensions not exceeding 62 inches. The contest consists of three flight missions and a ground mission that can be attempted any time during the contest. Flight missions must be completed in order with one additional attempt allowed for Missions 2, 3, and the ground mission to improve score.

Each flight mission consists of flying laps around the course depicted in [3.1](#). Missions start when the throttle is first advanced. The aircraft must then take off within 65 ft of the starting line and fly four legs: upwind, crosswind, downwind, and base. The upwind and downwind legs are both 1,000 ft long and centered about the starting line. The crosswind and base legs are both 180° turns. There is also a 360° turn at the midfield downwind position that must be completed. A lap ends when the aircraft passes over the starting line on the upwind leg. Finally, when the mission ends the aircraft must perform a successful landing, i.e., within runway bounds with no significant damage, for the mission to be scored. Before each flight mission, the flight crew has five minutes to load and secure the payload.

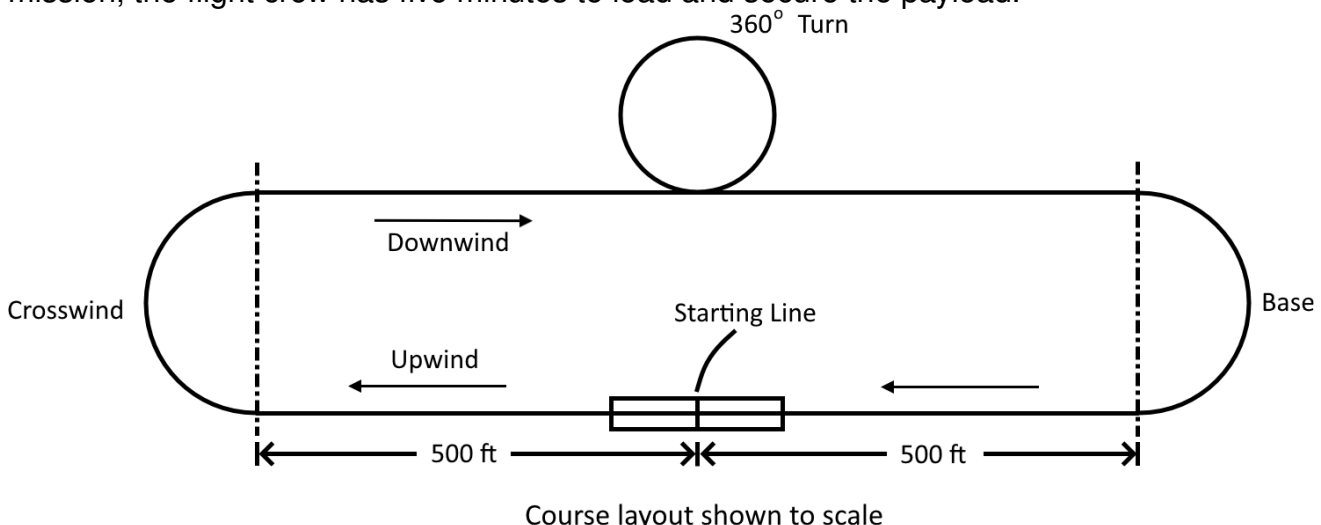


Figure 3.1 – Schematic of Course Layout. Adapted from AIAA [1]

3.1.1 Scoring Summary

Contest scoring is based on the below equation:

$$\text{Score} = \text{Written Report Score} \times \text{Total Mission Score} \quad (3.1)$$

The overall score depends entirely on the quality of this report (*Written Report Score*) and the combined scores of all missions (*Total Mission Score*). *Total Mission Score* is simply the addition of all mission scores as follows:

$$\text{Total Mission Score} = M_1 + M_2 + M_3 + GM \quad (3.2)$$

Values of M_1 , M_2 , M_3 , and GM are given in 3.1. Additionally, the table presents a brief overview of each mission.

Mission 1: Staging Flight This first mission does not require a payload and serves as a demonstration of the aircraft's stability and ability to fly in a controlled manner. The aircraft enters the staging box, with all its components inside the closed shipping box. In here, the teams will flip a coin twice to determine whether either wing set 1 or 2 will be used for that specific mission. Three laps must be completed within a five minute window. The time starts when the throttle is advanced for the first time and ends after passing over the starting line on the final lap. Additionally, the aircraft must take off within 60 ft of the starting line. Scoring for this mission is either a 1.0 (successful attempt) or a 0.0 (unsuccessful attempt).

Mission 2: Payload Delivery Flight Mission 2 serves to demonstrate the aircraft's ability to transport the electronic package. The payload for this mission is to weigh a minimum 30% of the empty weight of the aircraft. The team will again flip a coin twice to determine which set of wings will be used for the mission. The aircraft takes off within 60 ft and must complete as many laps as possible in 10 minutes. The scoring for this mission is the Electronics Package weight multiplied by the number of laps flown in that time window.

Mission 3: Jamming Antenna Flight For this mission, a Jamming Antenna will be mounted on the side of the aircraft wing tip opposite to the flight safety line in the direction of takeoff. The length of the Jamming Antenna is accounted for in scoring. The plane must take off within 60 ft, and the time window is five minutes. A total of three laps within the time window is required for team to be scored.

Ground Mission: Operational Demonstration The Ground Mission is a test of aircraft structural integrity, where teams enter the mission with all components and payloads inside a shipping

box. A coin is flipped twice to determine which wing set components will be used for the mission, and only the assembly crew member can touch the aircraft and payload. The assembly crew member has a ten minute window to assemble the aircraft and install the heaviest payload configuration, with the weight verified by the Ground Mission judge. The pilot will verify all flight controls are working properly, and the assembly crew member will install the structural test fixture onto the wing tips and apply test weights to the center of the aircraft fuselage until maximum weight is called or time expires. The mission score is determined by the total test weight divided by the maximum aircraft weight, with any structural failure or deformation resulting in a failed test.

3.2 Design Requirements

From the mission specification, relevant design parameters were chosen. A configuration was selected utilizing an approach that maximizes total mission score through analysis of the scoring parameters with the greatest impact.

3.2.1 Aircraft and Payload Constraints

While mission requirements constrain the design, it is further bounded by constraints imposed by the rules. Below are the restrictions put in place on the various components of the aircraft.

Aircraft Configuration

- 50 lbf shipping box weight limit
- Maximum sum of each dimension of the box has to be less than 62 inches.
- Shipping containers must be secured to prevent significant movement
- Two sets of removable wings, each labeled L1, R1, L2, R2

Payload

- Minimum 3in x 3 in x 6in box in length
- Minimum payload weight is 30% of the total aircraft weight

Jamming Antenna

- Unmodified 0.5 inch schedule 40 PVC pipe
- attached to the tip of each wing chosen by the AIAA personnel
- Can be of any length but no internal stiffening mechanism

Propulsion System

- Commercially available electric motors and propellers
- External switch to activate radio control system
- Nickel-cadmium (NiCd), nickel-metal hydride (NiMH), or lithium polymer (LiPo) batteries only
 - NiCd and NiMH
 - * Only commercially available packs or individual cells
 - LiPo
 - * Unaltered, commercially available
 - * May not exceed 100 Wh. total energy
 - * Fuse must be located near positive terminal
 - * If using multiple packs they must be identical, connected in parallel, and have a 0.25 in. gap between each battery
- Only one battery type is allowed

3.3 Score Sensitivity

The aircraft must be capable of being compactly stored, swiftly constructed, and fly various electronic warfare missions. The designed aircraft must perform three flight missions and one ground mission. Table 3.1 provides a summary of each mission requirement.

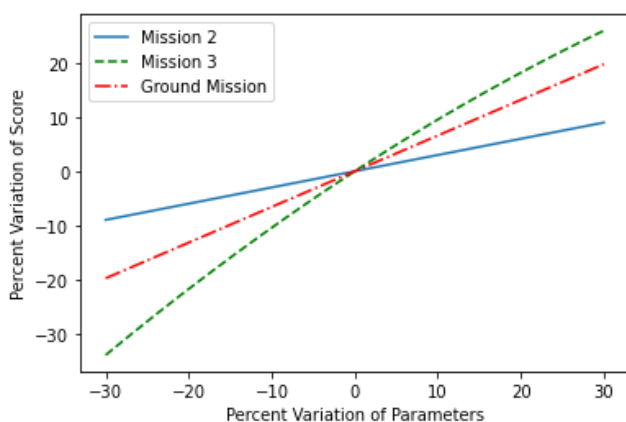
Table 3.1 – Mission Requirements and Subsystem Design

Mission	1- Test Flight	2-Assembly	3-Antenna Flight	4-Ground Mission
Requirement Summary	No payload. Complete 3 laps in 5 minutes.	Assemble the aircraft and fly as many laps as possible in 10 minutes. The electronics package must fly with the plane.	Fly 3 laps as fast as possible with the antenna attached.	Structural load testing, via wing-tip tes
Design Objective	Wing and propulsion system design must enable take-off in 60 ft. without EW payload and provide minimum 26 mph average flight velocity.	<ul style="list-style-type: none"> • Wing and tail boom assembly must be simple and be quick to build, allowing for more flight time. • Wing and tail must be secure during flight. • Wing and Propulsion design should maximize cruise velocity to achieve the highest amount of laps in the allotted time. • Tail control surfaces should have sufficient volume to manage the increased weight of Electronic payload and still perform attitude control duties. 	<ul style="list-style-type: none"> • Builds on M2's requirements. • Antenna must be mounted on wing. • Tail control surfaces should be capable of fixed deflection to counteract surplus drag and related moments caused by the antenna. 	<ul style="list-style-type: none"> • Structure should aim to maximize wing strength to weight ratio to allow for higher loading weight relative to aircraft weight
Scoring	$M_1 = 1.0$ (Successful)	$M_2 = 1 + \frac{(Laps \cdot W_{Payload})_{IT}}{(Laps \cdot W_{Payload})_{max}}$	$M_3 = 2 + \frac{(L_{antenna}/t)_{IT}}{(L_{antenna}/t)_{max}}$	$GM = \frac{(W_{total}/W_{max})_{IT}}{(W_{total}/W_{max})_{max}}$

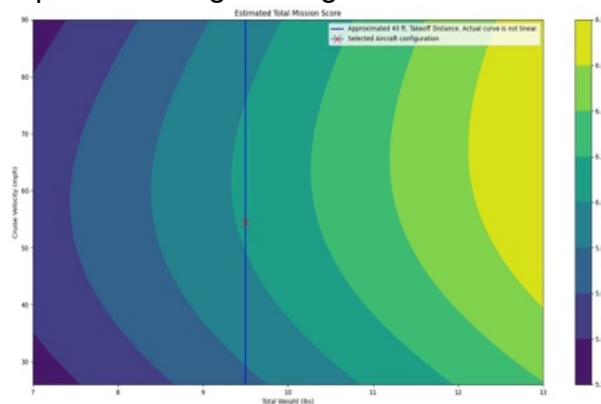
A sensitivity analysis was performed to determine the effect of design parameters on score. Based on Figure 3.2a and 3.2b it was found that a high thrust, high payload configuration is ideal for maximizing score. It was determined that a single motor, high-wing monoplane with a conventional tail would be the most stable and highest scoring configuration. The monoplane configuration was chosen due to its low drag, low weight, and ease of manufacture. A single motor was chosen to permit increased structural strength of the wing, necessary for the Ground Mission. A high wing configuration provides higher aerodynamic stability and increases propeller sizing options.

Additionally, Figure 3.2b relates the geometric parameters to minimum required thrust-to-

weight ratio (TWR). Here, the thrust to weight ratio is independent of wing loading, and the ideal lift coefficient is around 0.5-0.8 with highest possible wing loading.



(a) Parameter Score Variation



(b) Relating Critical Design Parameters. Line of 40 ft. Maximum takeoff distance is a linear approximation.

Figure 3.2 – Score Analysis

3.4 Configuration Selection

With score sensitivity analysis in mind, configuration selection was done by comparing various component options and selecting those which best represented the design parameter trends. The general process utilized a scoring system in which different configurations were ranked based on their relative superiority in various categories. Configurations were ranked from 1 (lowest) to N (highest), where N is the number of configurations considered. Each configuration's rank in every category was then multiplied by a pre-determined weight and summed. The configuration with the highest total score was then selected.

3.4.1 Wing Configuration

Since it was preferred to maximize wing loading, lift was chosen as the most important criteria. Weight, payload capacity, and drag were all of equal importance to overall aircraft performance. Finally, stability and ease of manufacturing were least important. Five different wing configurations were considered. The advantages and disadvantages are outlined below with a summary shown in Table 3.2.

Monoplane: The monoplane scored high on payload capacity, stability, and ease of manufacturing. In addition, its low weight and average drag were preferable.

Biplane: The biplane has high lift and an acceptable payload capacity. Its heavy weight, sub-par drag, stability, and difficult manufacturing were not a preferable option.

Tandem Wing: Tandem wing scored well in drag and stability while having below average scores in weight, lift, ease of manufacturing, and drag.

Blended Body: The blended body configuration scored well in lift and ease of manufacturing, but poorly in weight, drag, and stability. Payload capacity had an average score.

Flying Wing: A flying wing has low payload capacity and poor stability. Low weight and low drag were positive traits taken into consideration.

Table 3.2 – Wing Configuration Selection Matrix

Criteria	Weight	Monoplane	Biplane	Tandem Wing	Blended Body	Flying Wing
Lift	25	1	5	2	4	3
Weight	20	4	2	3	1	5
Payload Capacity	20	5	4	2	3	1
Drag	20	3	1	4	2	5
Stability	10	5	3	4	2	1
Ease of Manufacture	5	5	3	1	4	2
Total	100	340	310	275	260	315

3.4.2 Motor Selection

Propulsion requirements were determined from the desired thrust-to-weight ratio and endurance. The required thrust for takeoff and cruise speeds were determined based on the aerodynamic parameters and structural limitations of the preliminary aircraft design. Each configuration was simulated in the eCalc online propulsion tool, with a 15 x 10 inch propeller, 5000 mAh 5 cell Lithium Polymer (LiPo) battery, and 60A Electronic Speed Controller (ESC), and evaluated for flight time, thrust-to-weight, and total weight. Each configuration was also evaluated for thermal and electrical safety ie. motor over rated wattage, current does not exceed ESC rated current, estimated motor temperature.

Criteria	Points	Power 60A	SII-4020	X5-400
T/W	45	3	1	2
Flight Time	30	2	3	1
Weight	35	2	1	3
Total	100	265	170	225

Table 3.3 – Propulsion Selection Matrix

3.4.3 Wing Location

Placement of the wing contributes to several effects that are important to all stages of flight. First, and most importantly, wing placement will have a significant impact on stability. Different wing locations will also enable various landing gear configurations to be considered. Ground effect will have a significant impact on low altitude performance—particularly with takeoff and landing distance. Different structural geometries will be required for each placement and affect the difficulty of manufacturing. Three different wing locations were considered. The advantages and disadvantages are outlined below and summarized in Table 3.4.

Low Wing: The low wing location would be the least stable while having the best ground effect and ease of landing gear placement.

Mid Wing: Having a mid wing setting has overall median scores in stability, ground effect, landing gear placement. It is the most difficult to manufacture.

High Wing: The high wing placement would lead to the best stability and ease of manufac-

turing. It has the most difficult landing gear placement and poor ground effect.

Table 3.4 – Wing Location Matrix

Criteria	Weight	Low Wing	Mid Wing	High Wing
Stability	50	1	2	3
Landing Gear	20	3	2	1
Ground Effect	15	3	2	1
Ease of Manufacture	15	2	1	3
Total	100	185	185	230

3.4.4 Tail Configuration

The tail of the aircraft presents several design considerations that will have a major impact on aircraft performance. Most important were the structural integrity and stability provided by the configuration. Additionally, it was nearly as important to have a configuration that allowed for appropriate control authority. Again weight was a point of consideration. A rather unique criterion was the configuration's expected behavior at higher angles of attack which is particularly important during takeoff, landing, and gusting conditions. Ease of manufacturing was a point of concern. Five different tail configurations were considered. The advantages and disadvantages are outlined below and summarized in Table 3.5.

Conventional: A conventional tail provides excellent stability and control, while allowing for light weight construction and ease of manufacturing. Possible issues with vorticities from the wing or fuselage affecting control surfaces.

T-Tail: An advantage of the T-tail is keeping the elevators out of the disturbed airflow from the wing and fuselage. This also allows for improved glide ratio. However, due to the elevator being above the vertical stabilizer, this requires the stabilizer to be stronger, leading to increase weight due to the added support. The T-tail scored well for controls but scored average or below average for all other factors.

H-Tail: An H-tail allows for the vertical stabilizer to be free from the parasitic drag produced by the fuselage and has reduced stress at the root. The two vertical stabilizers cause a heavier and stronger root, causing manufacturing and design complications. H-tail scored well in AOA performance, rigidity, stability, and weight, while scoring low in controls and ease of manufacturing.

Twin Boom: An advantage of a boom mounted tail is that it allows for a large payload capacity and large tail surfaces. Disadvantages include the drastic increase in weight and drag due to boom design. Having the elevator between the two vertical stabilizers would be less effective than a conventional design due to the disturbed airflow from the fuselage.

Ring Tail: The major advantage of the ring tail is stability due to a large surface area to control both vertical and horizontal axes. A disadvantage is the drag, difficulty of manufacturing, and



the complexity of implementation and design of a ring tail.

Table 3.5 – Tail Configuration Matrix

Criteria	Weight	Conventional	T-Tail	H-Tail	Boom-Mounted	Ring-Tail
Rigidity	30	5	2	4	3	1
Stability	25	5	2	4	1	3
Controls	20	5	4	2	1	3
Weight	10	5	3	4	1	2
AOA Performance	10	4	1	5	2	3
Ease of Manufacture	5	5	2	3	4	1
Total	100	490	240	365	185	220

3.4.5 Landing Gear Configuration

The advantages and disadvantages are outlined below and summarized in Table 3.6.

Tricycle: The Tricycle landing gear was selected due to its superior handling capacity as well as anticipating sensor deployment/recovery operations while remaining cognizant of the need for ease of manufacturing. This landing gear was determined to be straightforward in assembly, despite its lower drag and higher weight disadvantages.

Tail-Dragger: The conventional landing gear scored best with its low drag capabilities and light weight. It produces less parasitic drag due to its placement further from the center of gravity, which supports a smaller portion of the overall aircraft weight and resulting in its capacity to be made smaller and lighter.

The Tail-Dragger is most susceptible to "nose-over" and thus scored low in handling capabilities. The sensor's deployment/recovery were considered in configuration determination and was predicted to be hindered by a conventional landing gear as well as being more complex to manufacture.

Table 3.6 – Landing Gear Configuration Matrix

Criteria	Weight	Tricycle	Tail-Dragger
Handling Characteristics	30	2	1
Deployment Reliability	25	2	1
Ease of Manufacturing	20	2	1
Drag	15	1	2
Weight	10	1	2
Total	100	175	125

3.5 Propulsion Sizing

eCalc, a propulsion system analysis software, was used to find battery, propeller, and motor configurations that met the targeted thrust, cruise speed, and endurance requirements. A selection matrix was used to determine the motor for the aircraft, shown in Table 3.3. All configurations are predicted to have a thrust-to-weight ratio above 1.00 and mixed flight time of at least ten minutes. These motors or an equivalent KV motor were then found and tested

with several configurations discussed in Testing. A thrust-to-weight target of 1.00 was chosen to provide flyable thrust levels, while still providing capable acrobatic performance for missions 2 and 3. The ten minute mixed flight time target was chosen to allow for full utilization of time in mission 2, the longest duration flight. All of the motors in consideration were purchased and tested in Section 7.

A multi motor configuration was considered, but deemed too difficult to smoothly integrate with a detachable wing system. Additionally, the ground mission does not aid the wing-mounted configuration. A pusher-puller was also considered, but rejected for packing and payload spacial concerns. A ducted fan design was not used as wing mounting was undesirable and fuselage integration would limit payload options.

3.6 Wing and Jamming Antenna Integration

With the requirement of detachable wing sections designed for rapid assembly and high structural strength, a fast attachment method was necessary for mounting the wings. Side mounting of the wings was chosen to maximize available wingspan and allow for ease of wing section manufacturing. Each wing will be mounted by sliding the two wing spars into two hollow shafts in the fuselage. Locking pins will secure the wing to the fuselage while allowing for strong structural coupling. Similarly, the antenna (see Figure 3.3) will be mounted using a 3D-printed component that will slot into the hollow carbon fiber spars at the wingtips. A counterweight will be used on the opposite wingtip to improve lateral stability.

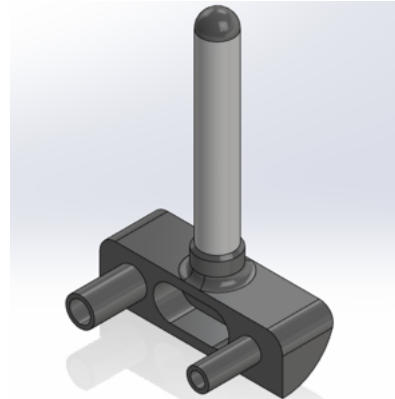


Figure 3.3 – Antenna

3.7 Final Results

The final design will be a high-wing, conventional monoplane with a single mount motor. It will also utilize a tricycle landing gear with conventional tail design. This configuration ensures that the aircraft will have high speed and payload capacity. Additionally, manufacturing should be relatively simple.

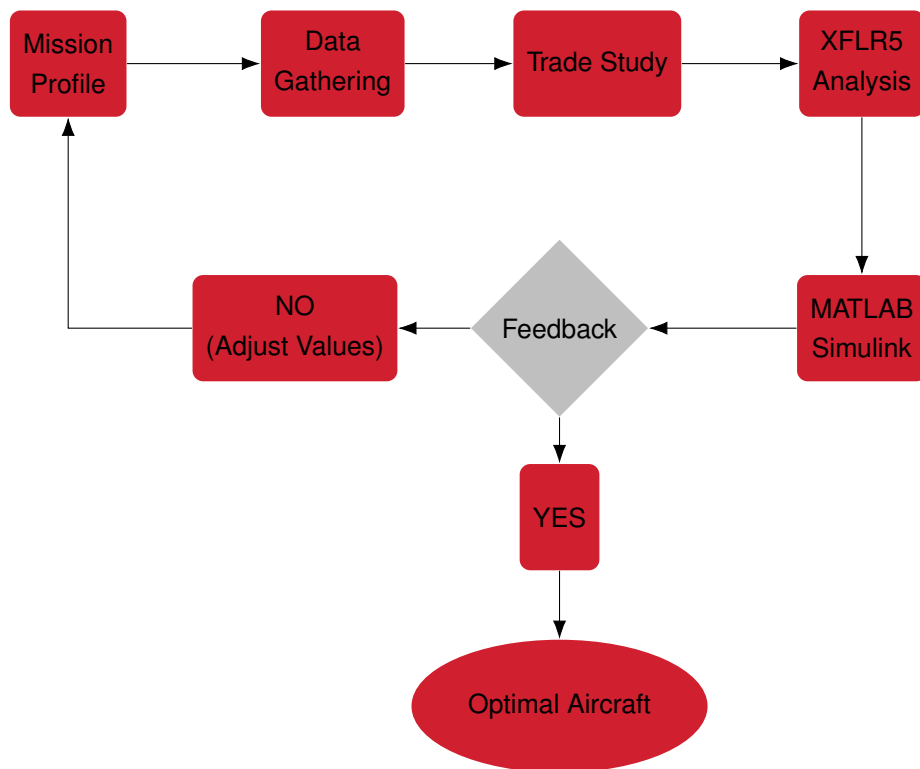
4 Preliminary Design

4.1 Description of Design Methodology

To ensure our project results in an effective and efficient aircraft, we have made a project plan to provide the best output parameters (Figure 4.1). After reviewing initial mission definition and requirements, numerical studies were conducted. Firstly, data for existing RC aircraft was collected. This data will be used to compare performance metrics of Goon-Hawk with existing planes. Once design metrics, such as maximum wing size from box dimension, thrust to weight ratio, mission lap time, take off weight, and wing loading are selected, Python scripts, sizing matrices and other methods will be used to plot the data for analysis. We then proceed

to study the aerodynamic properties of the aircraft via XFLR5, a software that can perform airfoil analysis and to simulate/analyze the behavior of a specific aircraft design under a certain set of conditions. After reading the feedback, we plot the data using Matlab Simulink. If the findings are feasible, we proceed to component design phase and if not, refine our mission definition and operational requirements. This is an agile project managing system where select the performance parameters and perceive the coverage, operation orbit and bypass simultaneously to decide the best fit. This allows us to be flexible with the limited time provided for this project.

Figure 4.1 – Design and Analysis Methodology



For a detailed project flow chart, Figure 4.2 lays out the plans followed for the development, manufacturing, and testing phase.

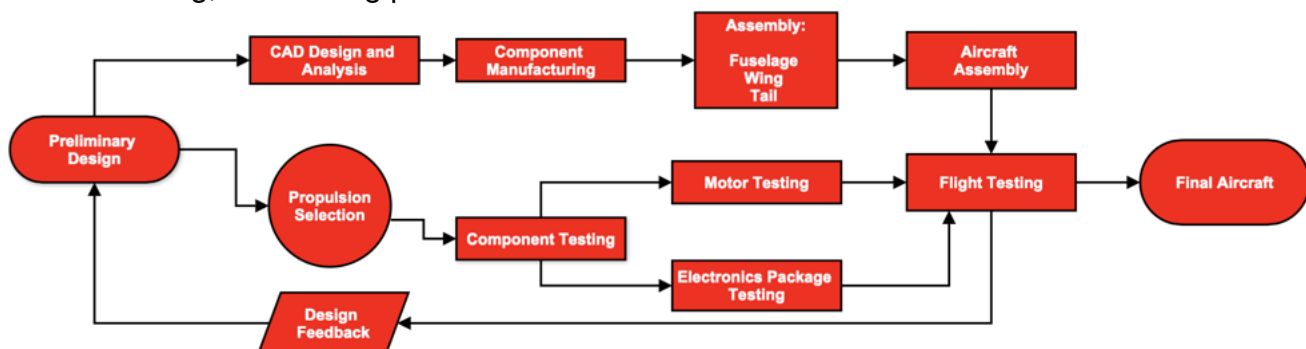


Figure 4.2 – Project Plan Flow Chart

4.2 Box Sizing Trade

The primary constraint for this project is the shipping box. The team looked to maximize the volume of the box, resulting in a larger set of wings, larger fuselage, and thereby maximum allowable payload for Mission 2. To estimate the box sizing a partial differential equations was utilised as follows:

To maximize the box volume, subjected to the given constraint where the dimensions add up to 62 inches we start with Equation (4.1) and (4.2) as:

$$V = L * W * H \quad (4.1)$$

$$L + W + H = 62 \quad (4.2)$$

Using the method of Lagrange multipliers [6], the Lagrangian function is:

$$L = L * W * H + \lambda(L + W + H - 62)$$

Taking the partial derivatives with respect to L, W, H, and λ , we set the following boundary conditions:

$$\frac{\partial L}{\partial L} = WH + \lambda = 0$$

$$\frac{\partial L}{\partial W} = LH + \lambda = 0$$

$$\frac{\partial L}{\partial H} = LW + \lambda = 0$$

$$\frac{\partial L}{\partial \lambda} = L + W + H - 62 = 0 \quad (4.3)$$

Solving Equation 4.3 using Python PDE script we get Graph 4.3 shown down below. The predicted graph show two peak lines, that correspond to the maximum dimensions of the box. Those two dimensions can be:

$$22.5 \leq W = L \leq 27.5$$

Therefore, we can compute the third dimension easily as follows:

$$H \leq 62 - L - W$$

Based on these values, the team decided the dimensions that could potentially result in maximizing plane performance subject to the constraint are $L = 26.5$, $W = 24$ and $H = 11.5$.

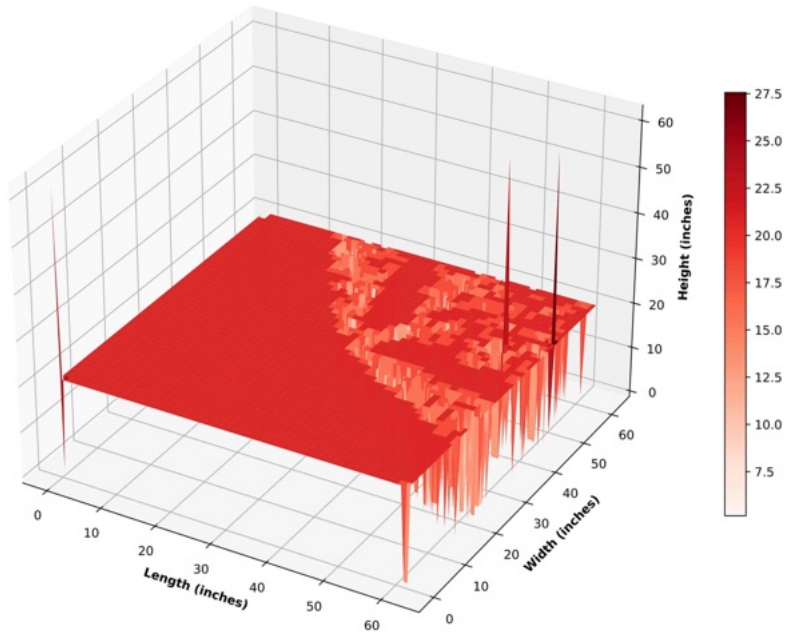


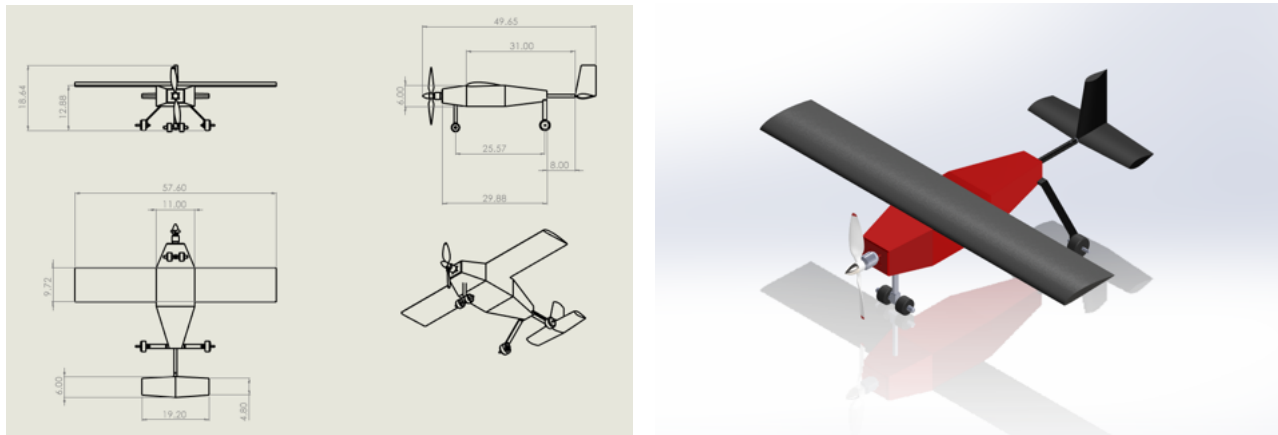
Figure 4.3 – Optimal Box Dimensions

4.3 Preliminary Aircraft Sizing

Wing and tail dimensions were determined using XFLR5, an X-FOIL-based aircraft design and analysis software. The maximum wing span of 4.8 ft according to box dimensions was selected with a rectangular wing planform and chord of 9.7 in. The main wing incorporates the Clark Y airfoil, as XFLR5 analysis showed that this airfoil produced the least drag during cruise conditions. It also produced the most desirable stability characteristics of the airfoils analyzed. With the current aircraft's total weight and wing area, the wing loading is approximately 2.5 lbs/ft². A conventional tail configuration was selected for the tail section. Using the dimensions of the main wing and historical data, the horizontal and vertical stabilizers were sized. The horizontal stabilizer has an area of 115 in² and uses a NACA 0012 airfoil, and the vertical stabilizer area is 44.7 in² with a NACA 0012 airfoil. The static margin was calculated at 22.9% with the payload and 25.8% without allowing the aircraft to remain longitudinally stable despite differing centers of gravity for Missions 1 and 2.

4.3.1 Alternative Sizing Solutions

After doing the preliminary aircraft sizing, the team went on to look other alternative based on relevant mission profile, and box dimension. Figure 4.5 shows three aircraft sizing's considered with different weights, and components. The team then selected the final design based on the performance metrics provided in the later section of the report.



(a) Aircraft Preliminary Sketch

(b) Aircraft Preliminary 3D-CAD

Figure 4.4 – Preliminary Design

Parameters	Units	Value	Alternative 1	Alternative 2	Alternative 3
MTGTO(W0)	lb	10.8	9.5	7.2	9.5
Thrust (T) Static	lb	12.81	12.5	7.704	12.656
T/W		1.18	1.31	1.07	1.332
V_cruise	ft/s	73.33	67		80.667
V_max	ft/s	88	96.8	85	96
V_TO	ft/s	35.2	51.92		53.24
V_stall	ft/s	32	47.2		48.4
V_approach	ft/s	38.4	56.64		58.08
Configuration		single @ nose	single @ nose	single @ nose	
Motor Type		E-Flight P-160	E-Flight P-90	Eflight Power 60B	EF-p60B-16x10
Motor Weight	lb	1.43	0.99208		0.8375
Mass Bat	lb	1.87	1.87	1.25	1.5625
Wing Area (S_A)	in^2	642	594	469	560
Chord	in	11.2	11		9.72
Thickness (t)	in	3	2.56		1.33
Full Span (b)	in	57.4	54	57.4	57.4
AR		5.13	4.91	6	6
tip C	in				9.72
W_struc	lb	4	3.4865	3.2	3.68125
W_prop	lb	3.63	3.135	2.16	2.96875
W_payload	lb	3.3	2.85	2.376	2.85
Wing Loading S	lb/ft^2	2.56	2.28805395	2.9	2.5

Figure 4.5 – Alternatives Considered

4.4 Aerodynamics Airfoils, Lift, Drag

4.4.1 Airfoils

To select the airfoils, XFLR5 software was used to analyze the lift and drag, and ease of manufacturing was considered. For stability, it is best to use a symmetric airfoil for the vertical and horizontal stabilizers, and cambered for the wings. Based on the data shown in Table 4.1 and the shapes shown in Figures 4.6 and 4.7, a Clark-Y airfoil was chosen for the wings and

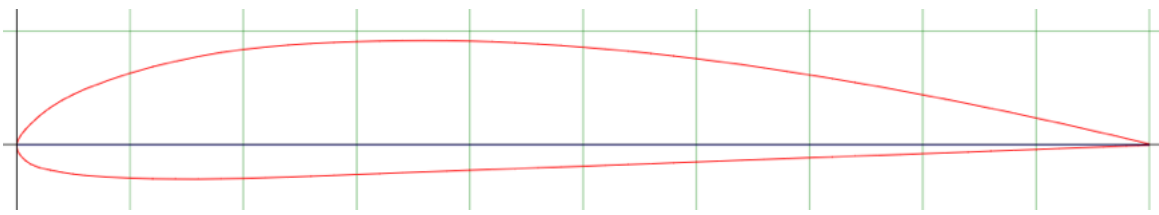


Figure 4.6 – Clark-Y Airfoil

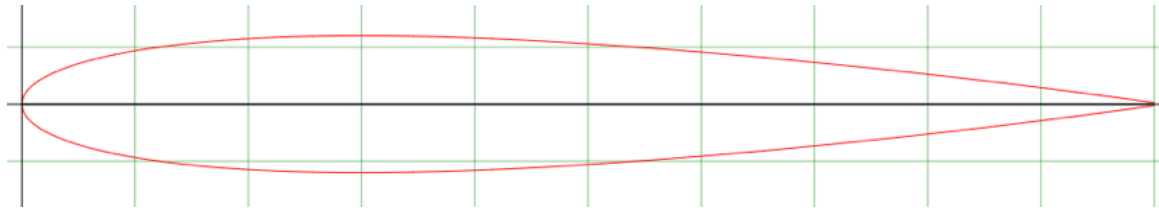
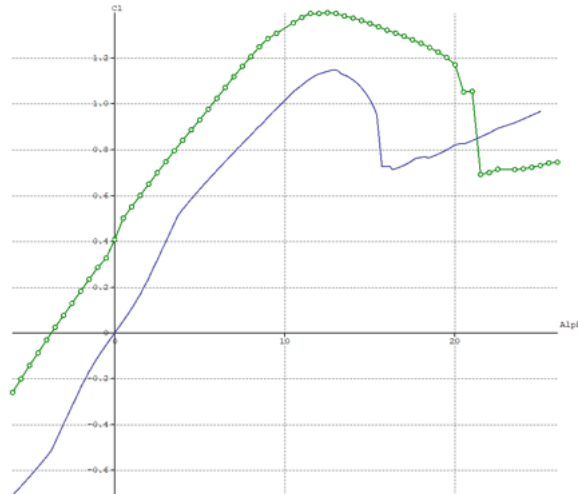
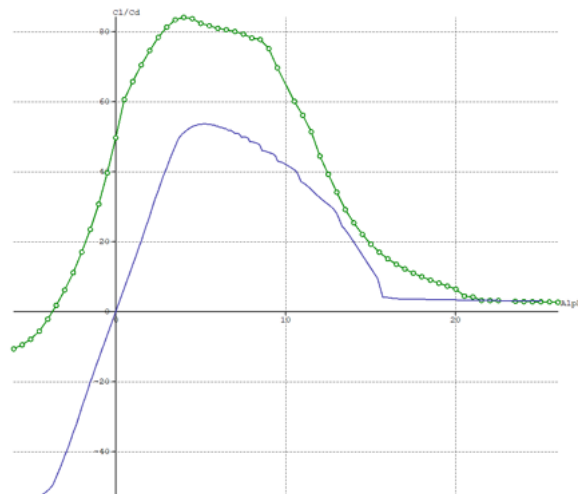


Figure 4.7 – NACA 0012 Airfoil

Figure 4.8 – C_l vs. α of AirfoilsFigure 4.9 – C_l/C_d vs. α of Airfoils

a NACA 0012 for the tail. Figures 4.8 and 4.9 are the XFLR5 graphs from which the data was collected [2]. The airfoils were analyzed at Mach .15 and a Reynolds Number of 300,000. The green line is the Clark-Y airfoil and the blue line is the NACA 0012 airfoil.

Table 4.1 – Airfoil Characteristics

	NACA 0012	Clark-Y
$C_{l_{max}}$	1.1 @ $\alpha = 12.9^\circ$	1.4 @ $\alpha = 12.2^\circ$
Max C_l/C_d	53.1	83.8
C_{l_0}	0	0.4
α @ $C_l = 0$	0°	-3.7°



4.4.2 Lift

To calculate lift, XFLR5 data was used in conjunction with equations 4.4 and 4.5.

$$C_L = C_{L_0} + C_{L,\alpha} * \alpha \quad (4.4)$$

Where C_L is the overall lift coefficient, C_{L_0} is the lift coefficient when $\alpha = 0^\circ$, and $C_{L,\alpha}$ is the slope of the lift curve.

$$L = C_L \frac{\rho V^2 S}{2} \quad (4.5)$$

Equation 4.5 is the standard equation for lift in which S is the area of the wing, ρ is the density, and V is the velocity. The velocities used in calculations are what it was determined the aircraft would safely be able to fly at based on XFLR5 data. Table 4.3 shows the lift predictions by mission.

4.4.3 Drag

Friction drag is expected to be low because MonoKote has a low coefficient of friction [5]. Induced drag will only be an issue on takeoff and around turns, but that is inevitable from generating lift. The airfoils and the aircraft shape were chosen in part because they do not cause high drag, so while there will be some form drag, it should be minimal. Induced drag will also increase during flap deployment, but as flap deflection is only used during takeoff and landing, expected overall drag performance is assumed to be low.

4.5 Aircraft Stability

4.5.1 Static Stability

The static margin of the plane is calculated using Equation 4.6 from the planes preliminary dimension as:

$$SM = \frac{X_{NP} - X_{CG}}{C_{MAC}} * 100 = \frac{5.309 - 4.174}{9.602} * 100 = 11.82\% \quad (4.6)$$

This value found above indicates a stable aircraft with good predicted performance. This static margin can be improved further by CG adjustment. The wing incidence angle was set to 3 degrees, and similarly the elevator incidence angle used for the test was set to -2 degrees. The aircraft CG was placed at the quarter chord location of the main wing. To check static stability a negative slope C_m vs α graph (see Figure 4.10c) is required, along with a positive Trim angle. For Missions 1, 2, and 3 a positive trim angle of 5.4, 2.2 and 5.6 were obtained respectively. This indicates that the airplane is statically stable in all missions. Additionally, Figure 4.10d confirms that the airplane has a positive lift coefficient at the trim angle for each missions. A further break down of lift and drag is shown in Figure 4.10a.

To determine directional stability, a Type 5 analysis can be used to plot C_n vs Beta and examine the slope ($\frac{dC}{d\beta} > 0$). From graph 4.10b a positive slope is observed, and thus the airplane has

a restoring yaw moment which makes it directionally stable.

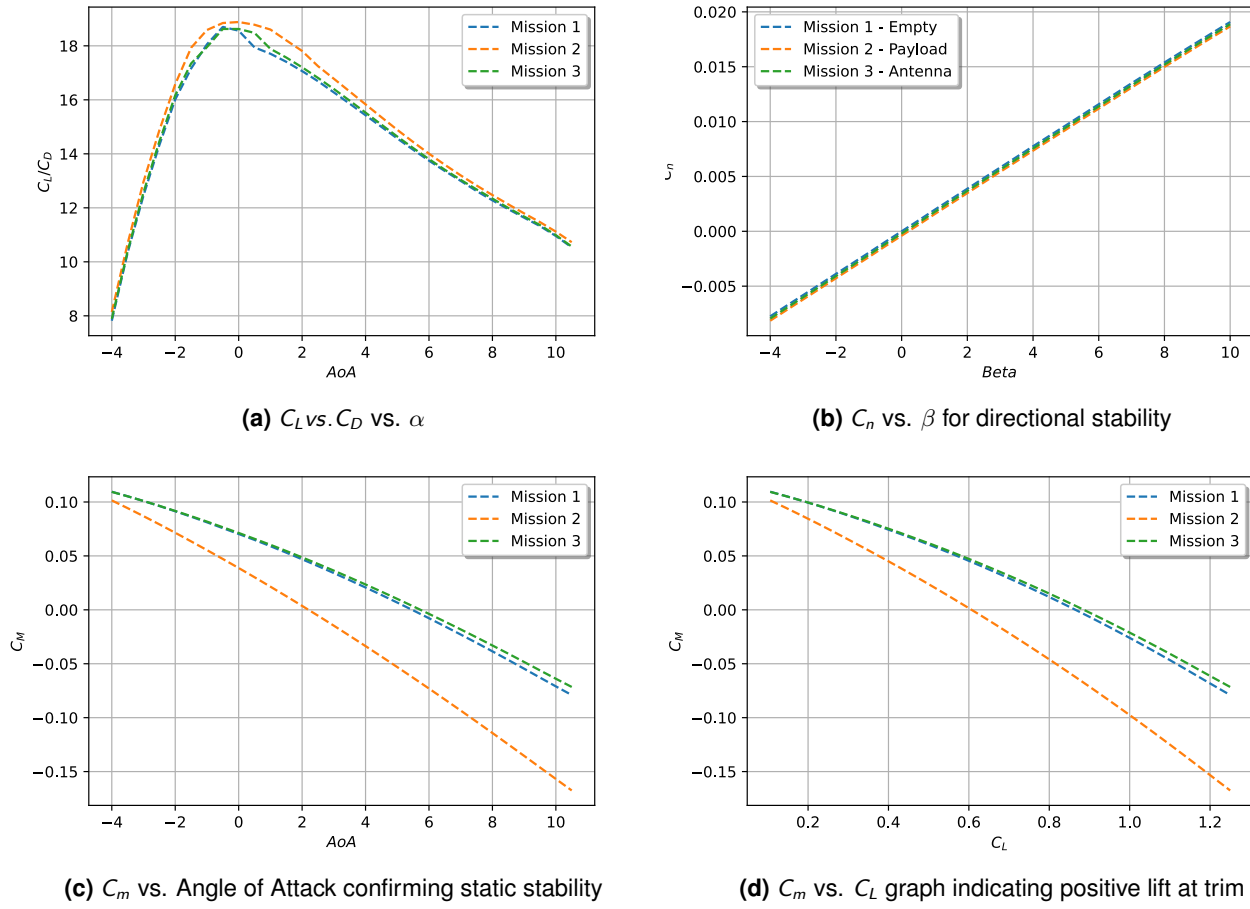


Figure 4.10 – Aerodynamics Analysis

4.5.2 Dynamic Stability Performance

Dynamic stability is one of the key factors that affect the flight performance of an aircraft. In XFLR-5, dynamic stability is determined by analyzing the aircraft's response to various flight conditions and disturbances. This includes analyzing the aircraft's pitch, roll, and yaw behavior under different flight conditions. XFLR-5 can also predict the aircraft's response to gusts and turbulence. Through this analysis, XFLR-5 can determine the aircraft's dynamic stability and provide recommendations for improving it.

Table 4.2 – Dynamic Stability Settings

Parameter	Value
Type 7:	Dynamic Stability
Method:	3D-Panels/VLM2
Inertia Model:	Plane Inertia
Mass:	7.175 lb
COG.X:	4.174 in
COG.Z:	-2.275 in
I_{xx} :	746 lb.in ²
I_{yy} :	322.4 lb.in ²
I_{zz} :	1033 lb.in ²
I_{xz} :	13.92 lb.in ²
B.C.:	Dirichlet
Analysis type:	Viscous
Ref. dimensions:	Planform
Ref. area:	494.400 in ²
Ref. span:	51.500 in
Ref. chord:	9.600 in
Density:	1.236 kg/m ³
Viscosity:	1.5e-05 m ² /s

Longitudinal Dynamic Stability In Figure 4.11a the analysis shows 4 root locus of the 2nd order oscillation. The left 2 are for short period and right 2 for long period oscillation. All those root are on the left side of the real axis line indicating longitudinally-dynamic stable.

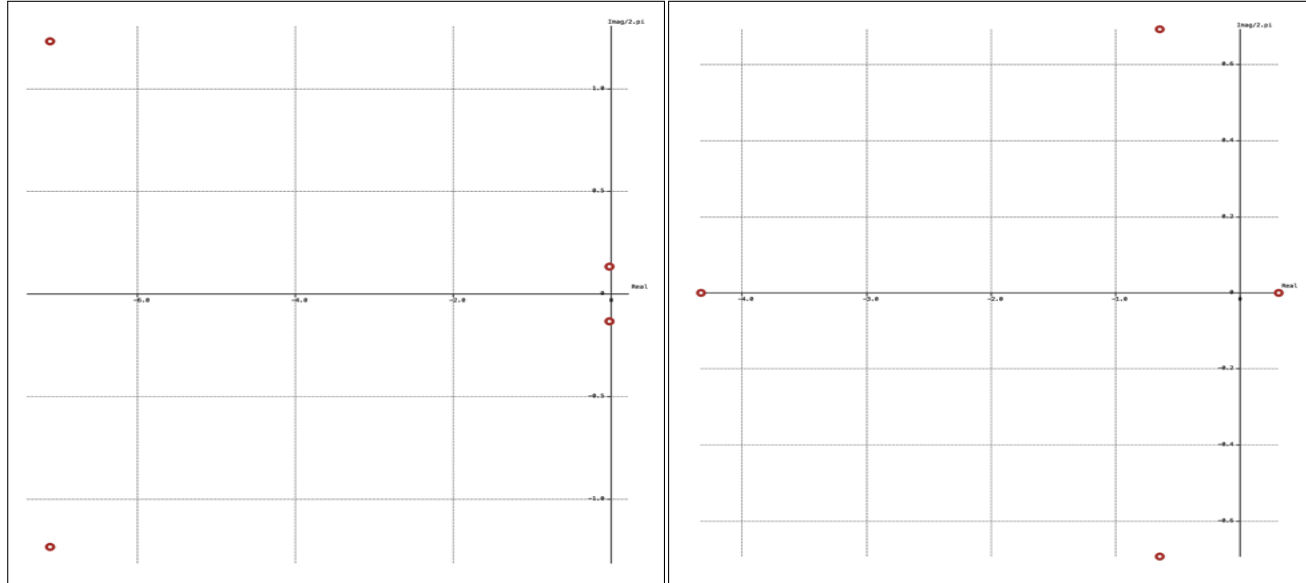
Lateral Dynamic Stability Similarly Figure 4.11b the analysis shows 4 root locus which correspond to the dutch roll and spiral modes. This concludes that the airplane is laterally-dynamic stable in the lateral direction. This meant that the airplane can operate without having to require a controlled input, will restore back to stable position if it encounters any force in the 3-axis.

Time response are used to analyze the dynamic stability of an aircraft. A Bode plot is a graph that shows the magnitude and phase of the aircraft's response to changes in its angle of attack or elevator deflection as a function of frequency [5].

The phase plot in 4.11c indicates how the amplitude of the aircraft's response changes with frequency for the dutch roll effects. It can indicate whether the aircraft has a tendency to oscillate or become unstable at certain frequencies. The phase plot shows the delay between the input and output signals, which indicates the aircraft's ability to respond quickly to changes in its angle of attack via elevator deflection. In this for $\pm 15^\circ$ deflection, it can be seen that the airplane returns to the neutral position after 4, 4.5, 6 seconds for Missions 1, 2, and 3 respectively.

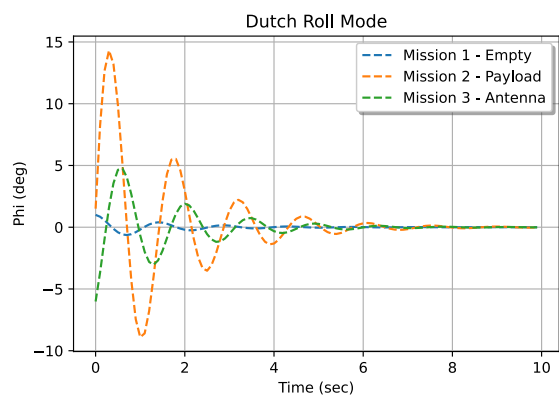
In general, a well-designed aircraft will have a Bode plot that shows a stable and well-damped

response to changes in angle of attack or elevator deflection across a wide range of frequencies. Figure 4.11d shows that if the Bode plot shows instability or excessive oscillation at extremely high frequencies, it will take no longer 170 seconds to bring itself back to the neutral position.

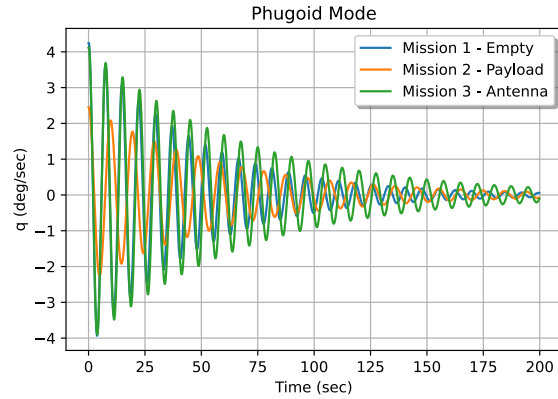


(a) Longitudinal root locus.

(b) Lateral root locus.



(c) Dutch roll time response.

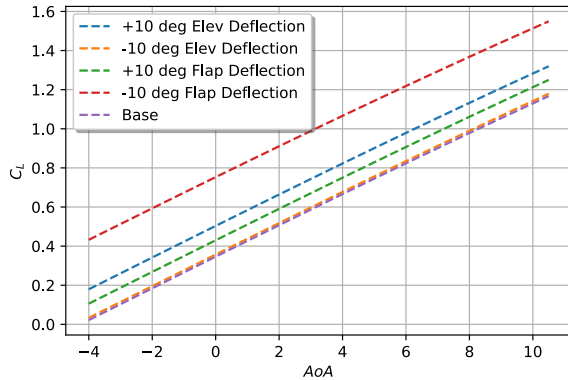
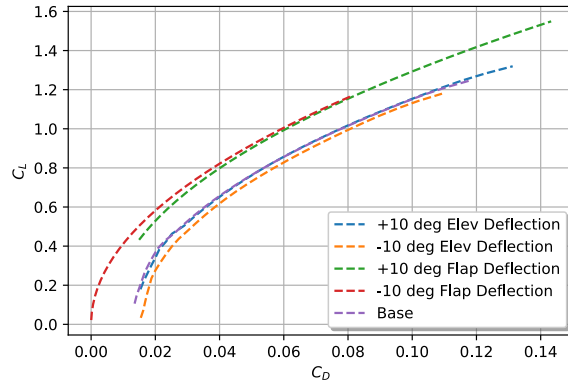


(d) Phugoid time response

Figure 4.11 – Dynamic Stability

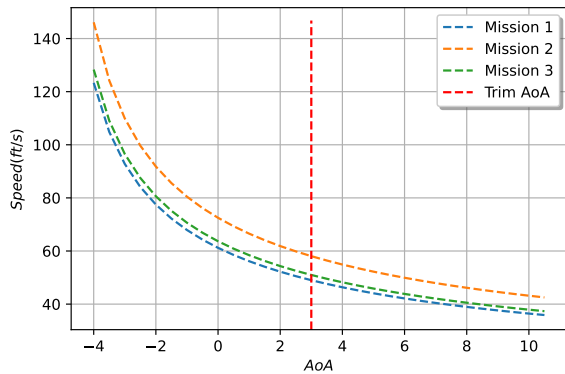
4.5.3 Control Surface Effects on Stability

Another performance metric the team explored was the effect of control surface deflection. Figure 4.12a shows the amount of lift coefficient gained by deflecting the elevator and flaps of the plane for only 10° . This in return corresponds to sizing the control surfaces in order to generate enough lift at a reduced speed. However, it should be noted that a small drag is introduced to operate at a higher lift coefficient (see Figure 4.12a).

(a) C_L vs. AoA for 10° deflection(b) C_L vs. C_D for 10° deflection**Figure 4.12 – Control Surface Effects across all Missions**

4.6 Estimated Aircraft Mission Performance

Each mission was simulated using the same assumptions and parameters used in the score analysis, namely using an air density taken from historical data near the Tucson fly-off site in April. Mission 2 assumed a maximum of 13 laps completed with a 3.25x3.2x6in payload package weighing 2.13lbs. The Mission 3 score assumed one jamming antenna placed in one side of the wing, with a counter weight attached on the other side. The predicted result is 3 laps completed in 1.5 minutes. The velocities used in calculations are what it was determined the aircraft would safely be able to fly at based on the XFLR5 data. Figure 4.13 shows the speed the airplane should fly in order to get the desirable scores. And those speed settings will generate us enough lift as shown in Table 4.3. This table contains the lift predictions for each mission. Finally the results from the simulated missions, predicted scores and preferred values are outlined in 4.4 below.

**Figure 4.13 – Estimated Speed Variation Across Missions****Table 4.3 – Speed Lift Predicted by Mission**

Mission	Cruise Velocity (ft/s)	Lift Cruise (lbf)
Mission 1	61	6.64
Mission 2	72.4	9.31
Mission 3	63.6	7.17

**Table 4.4 – Estimated Mission Performance and Predicted Scores**

Parameter	Mission 1	Mission 2	Mission 3
$C_{L,\max}$ [-]	1.40	1.40	1.40
$C_{L,\text{cruise}}$ [-]	0.67	0.73	0.62
e [-]	0.98	0.99	0.97
C_{D0} [-]	0.02	0.02	0.02
L/D_{\max} [-]	16.84	18.10	17.68 (5.33)
L/D_{cruise} [-]	16.53	17.19	17.67 (2.97)
W/S [oz/in ²]	19.39	34.75	27.07
v_{cruise} [ft/s]	38.9	49.9	47.4
v_{stall} [ft/s]	29.5	39.4	34.8
Gross Weight [lbf]	7.1	9.13	7.97
Mission Score	1.00	1.46	2.26

5 Detail Design

5.1 Structures Final Dimensional Parameters

The airframe dimensions did not vary between the preliminary and detailed design phases as structural analysis, propulsion tests, and aerodynamic analysis yielded ideal results. The final overall dimensions are shown below in Table 5.1.

Table 5.1 – Final Aircraft Dimensions

Fuselage	Wing		
Total Length	18.8 in.	Wingspan	51.5 in.
Nose Length	5.0 in.	Root Chord	9.60 in.
Empennage Length	3.0 in.	Tip Chord	9.60 in.
Width	5.0 in.	Mean Chord	9.6 in.
Height	4.5 in.	Aspect Ratio	5.365
Vertical Stabilizer		Planform Area	494.4 in. ²
Height	9.0 in.	Incidence	3 deg.
Root Chord	6.0 in.	Horizontal Stabilizer	
Tip Chord	3.0 in.	Span	21.98 in.
Mean Chord	3.38 in.	Mean Chord	5.15 in.
Tip Offset	3.0 in.	Incidence	-2 deg.
Distance from LE	30.8 in.	Distance from LE	31.2 in.

The structural components worked around volumetric constraints created by the aerodynamic design, based on the dimensions of the transport box. Areas with insufficient area for covering were reinforced with additional material, such as leading edge dowels, hardwood plates, and thin flexible wood material on the top surface.

5.2 Wing Design

As previously mentioned, a couple of critical parameters dictated the aircraft's wing design. The first is the rapid assembly of the wing sections to the fuselage during the various flight

missions. The second is a lightweight but strong airframe that can withstand the loads applied to the aircraft during flight and the ground-based load test.

The layout of the half-span wing is as follows: Two carbon fiber spars run down the wing's span and will be spaced at 2.4 inches from their centers, see Figure (5.1). Holding them in place will be eight Clark Y-shaped balsa wood ribs. Starting at the wing tip, these eight ribs will be placed along the carbon fiber spars approximately 3 inches apart. To improve the strength of the leading edge, a $\frac{1}{4}$ inch diameter wooden dowel spar will run down the wing span. In addition, a $\frac{1}{32}$ -inch thick balsa wood plate will lay across the wing at the leading edge. A backing plate will also be glued to the trailing edge of the ribs and will provide more strength and rigidity to the airframe. Hinges will be screwed into this backing plate which connects the flaperons to the rest of the wing. The flaperons, which have a chord length of 2 inches, span the entire length of the wing and are a simple but effective way of controlling our aircraft's motion. Additionally, hinge tape is the back-up solution for control surface mounting. Finally, the entire wing will be covered in MonoKote to provide the airfoil profile and minimize drag.

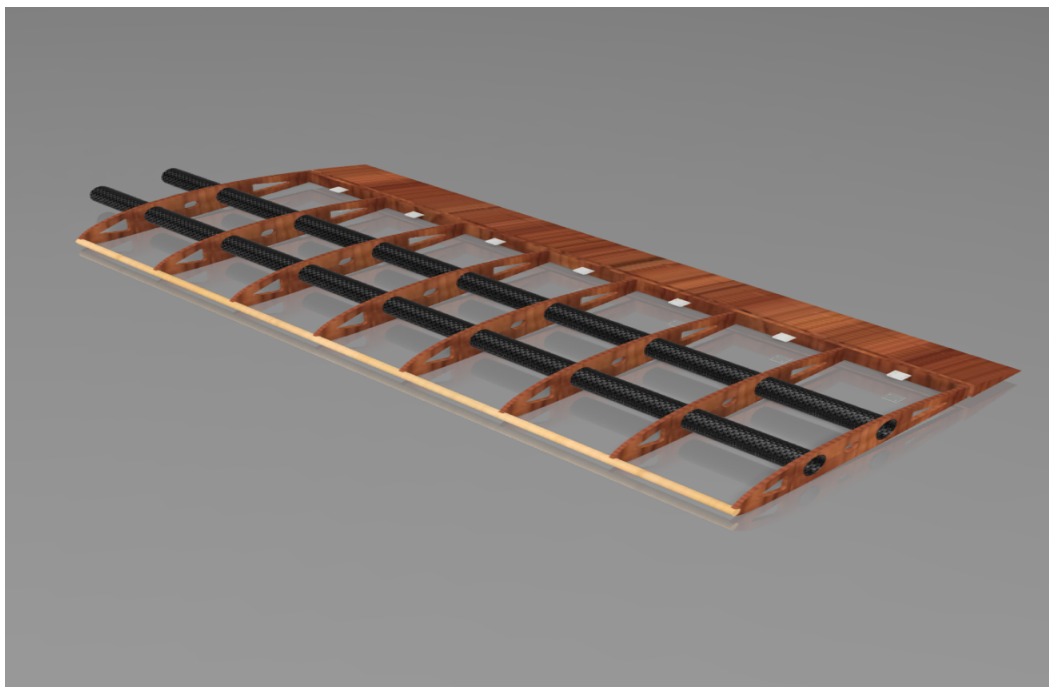


Figure 5.1 – Wing Detail Design

Due to the nature and requirements of this year's competition, the wings of our aircraft are divided into left and right half-span sections. During the competition, these wing pairs will be quickly attached by sliding the two carbon fiber spars into their corresponding hollow shafts located inside the fuselage. They will then be bolted or pinned together to prevent any movement or excessive vibration during flight.

To help minimize the structural weight of the wing, many of the materials used in this design are lightweight woods, such as $\frac{1}{8}$ inch thick balsa wood. However, the deliberate material

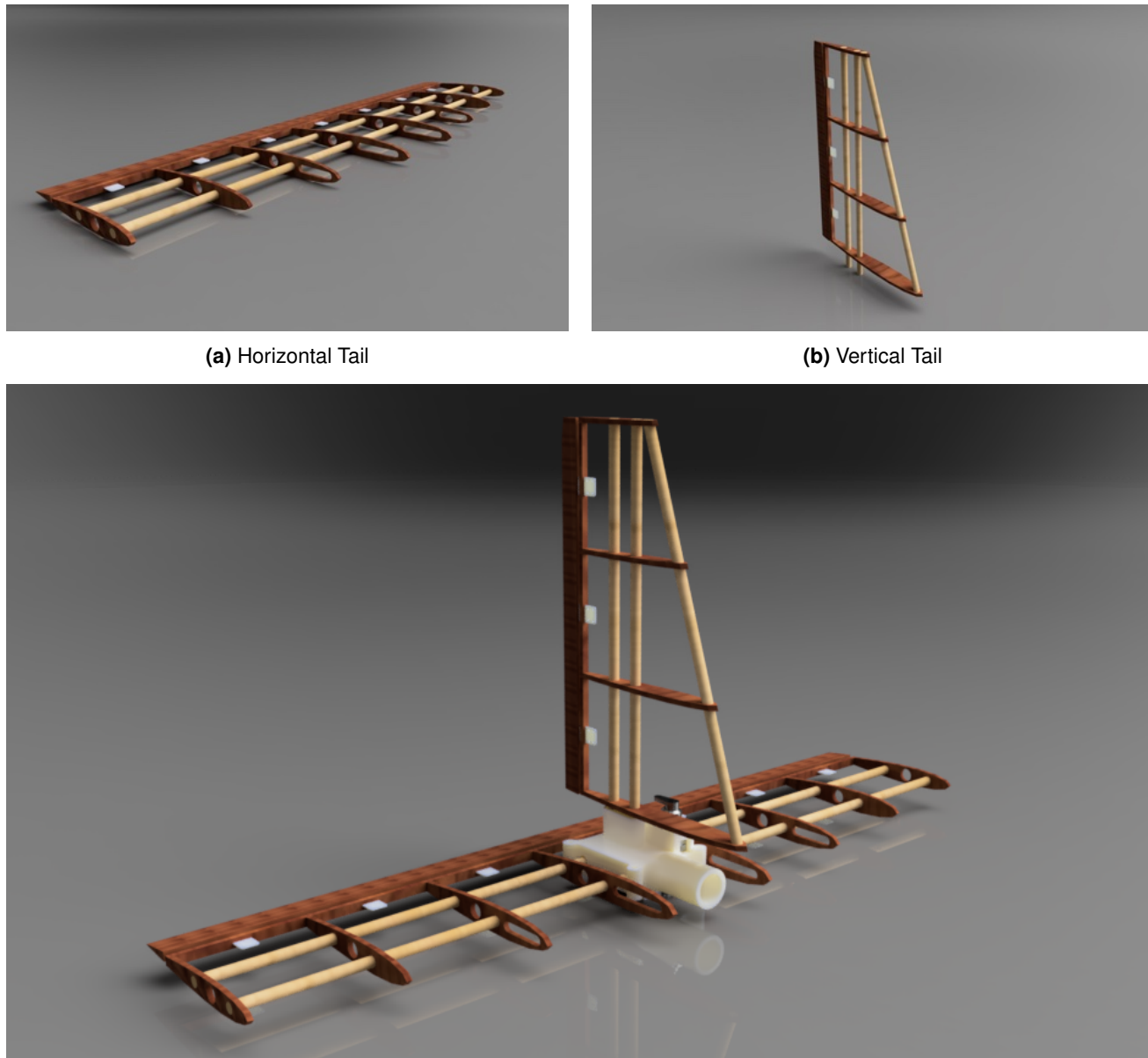
choice and placement of the wing spars ensured that any load experienced by the wing will be transferred to the carbon fiber spars, which can handle much higher loads than balsa wood. This spar load is then transferred into the fuselage section. This double spar configuration allows for excellent wing-tip loading performance, critical for the payload missions and the ground mission.

5.3 Antenna Design

One of the main objectives of this years competition is to be able to transport the largest antenna possible for the reconnaissance aircraft being designed. In order to do this, we had to find a method to quickly attach and adapt our antenna to the current flight conditions in order to obtain optimal flight performance. Upon collaboration with the team, it was decided that the desired method would be to 3D print an adaptor that slid into the spars of the wing sections. It is ideal to keep the adaptors mounted to the wing as it will take up little room in the box and be feasible to produce for all four wing sections allowing for our assembly time to be minimized. Furthermore, through the use of 3D printing the density of the print can be altered in order to offset the weight from the antenna to allow for optimum weights and balances. The design will rely on press-fits with close tolerances to ensure the adaptor and antenna do not back out of wing or the adaptor. Velcro may also be used to better secure the adapters to the wingtips. Refer to Figure 3.3 for the antenna adaptor design.

5.4 Tail Design

The tail of the aircraft includes a 22 inch elevator Figure 5.2a and a 9 inch tall rudder. The elevator and rudder are made up of laser cut balsa wood ribs sections that are held in place with $\frac{1}{4}$ inch wooden spar dowels. The rudder (see Figure 5.2b) also includes a reinforcement spar along its leading edge. The elevator and spar are mounted on a 3D printed 2 piece clam-shell which then is bolted to a 16 inch carbon fiber boom. This carbon fiber boom is then attached to the back end of the fuselage as seeing in Figure 5.2c.



(c) Horizontal and Vertical Tail Assembly

Figure 5.2 – Tail Detail Design

5.5 Fuselage Design

The fuselage of the aircraft is a single tapered segment made of $\frac{1}{8}$ inch thickness aircraft hardwood, with a $\frac{1}{4}$ inch motor plate, two $\frac{1}{8}$ inch bulkheads for the payload bay, 4 $\frac{1}{8}$ inch top mounted ribs, and a 3D-printed ABS tail connector. The top mounted spar was comprised of two 0.84 inch diameter carbon fiber rods with holes to allow for wing mounting. All fuselage components were joined with cyanoacrylate adhesive to ensure a secure fit. $\frac{1}{8}$ inch hardwood was chosen as the main fuselage material to provide a rigid structure for the high payload weight and spar force. Additionally, these thicknesses of wood were easily laser cut to allow for high precision and rapid prototyping.



Figure 5.3 – Isometric View

The aircraft was originally a 3-segment tapered design, thought preliminary prototypes had issues during manufacture and assembly with angled joints, low internal volume, and attachment complexity for the tail and landing gears. This design was then replaced with a single taper segment fuselage, narrowing to the tail. The advantages of this design were increased simplicity in design and manufacture and an elimination of the problematic high-angle joints from the conceptual design while still maintaining the structural rigidity and ease of manufacture via laser cutting. A consequence of this change from 3-segment to single taper is an increase in frontal drag due to the flat motor plate, though this can be mitigated via nosecone. Overall, the fuselage was changed in geometry to better accommodate manufacturing while sacrificing some aerodynamic efficiency. Additionally, the single segment improves load distribution across a larger face, further improving wing loading performance.



Figure 5.4 – Bottom View

An electronics bay access panel and payload bay panel were also cut. These are secured with Velcro strips to secure the flight electronics and payload respectively. The top rib sections allow for distribution of the wing spar load across the top plate of the fuselage, and the side panels are a single solid to increase strength for wing loading. The bottom of the fuselage also has areas for front and rear landing gear, with additional plates inside the fuselage for improved mounting seen in [5.4](#). There is an alignment hole in the rear bulkhead to allow for quick storage of the tail boom during transit and deployment. Finally, lightening holes were added to reduce the weight of the structure without sacrificing significant structural rigidity.

5.6 Landing Gear

The preliminary first design of the front landing gear consisted of a metal wire bent into a hole of the fuselage base that would loop around the wheel to act as an axle. Reconsideration of the materials used in this design was imminent due to the concern of reliability in the metal wire's structure and stability to stay on course.

The front landing gear needed to be removable and reassembled during the competition so a PVC pipe, diameter of 1 inch, with a PVC slip-on threaded male adapter coupled with a female adapter flange was used. A $\frac{5}{16}$ inch hole was drilled through one end of the PVC pipe perpendicular to the surface so a steel axle shaft can be threaded into. The wheel was slipped onto the axle shaft and locked into place while still being able to rotate easily by using a shaft lock collar. Dimensions of the shaft length was cut to $4\frac{3}{4}$ inches to ensure propeller blades stayed two inches above ground level. Fabrication of the female adapter flange consisted of a threaded PVC cap and a 3 inch diameter circle was cut from a $\frac{1}{8}$ inch thick piece of plywood using a drill press. The two pieces were epoxied together, and the PVC male adapter was epoxied to the PVC shaft holding the wheel. Three holes were drilled through the adapter flange and the base of the fuselage in an equilateral pattern for fasteners to hold the flange piece to the fuselage. The fasteners consisted of bolts, locknuts, and washers.

The design of the rear landing gear was a pre-bought aluminum alloy bowed and mounted to the base of the fuselage using three of the same fasteners in the front. The wheels were slipped onto the same aluminum shaft used for the front and locked into place using shaft lock collars.

A tricycle configuration is used for the landing gear. It consists of nose mounted and wing mounted wheels, encompassing the CG. This configuration was chosen to accommodate the payload bay. Both the front and back gear can be seen below in [Figure 5.6](#), and a summary comparing its functionality is shown in [Table 5.2](#).

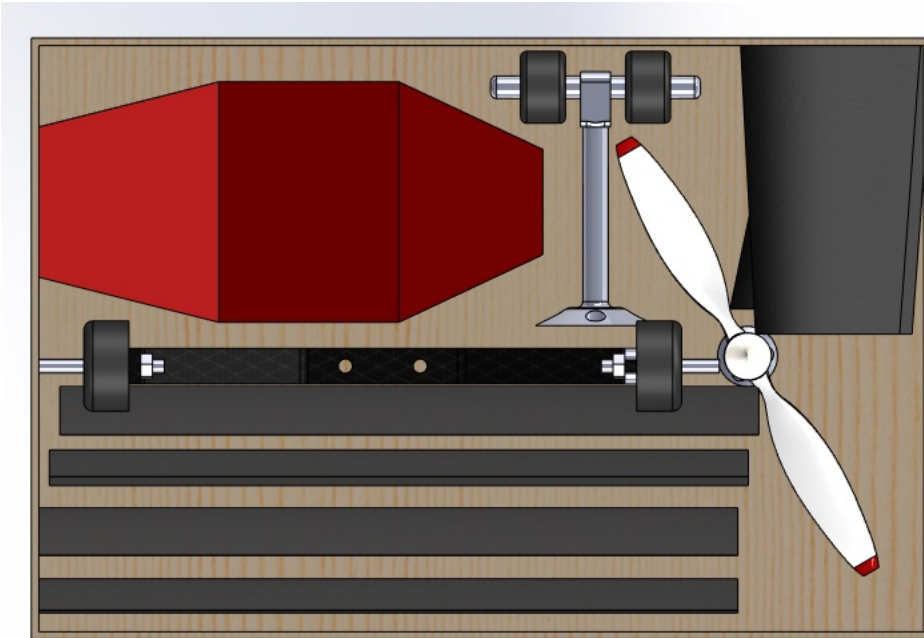
**Table 5.2 – Landing Gear Function Matrix**

Criteria	Weight	Fixed	Retractable
Drag	30	1	2
Weight	25	2	1
Complexity	25	2	1
Manufacturing	20	2	1
Total	100	175	125

Figure 5.5 – Landing Gear Design

5.7 Box Design

The purpose of the box is to transport all of the aircraft parts and what is needed to assemble them. The box is made out of 1/4" medium density fiber board (MDF), and was fitted together through the use of corner braces, screws, and wood glue. Holes were drilled in two sides to use as handles, latches were added to the lid to secure the lid, and a hinge was added to keep the lid attached. The dimensions are 26.5 x 24 x 11.5 in, which were picked based on dimensions of the aircraft and the requirement that the linear dimensions could not sum to more than 62 in. Before construction, a CAD model of the box was made with all parts inside to be sure everything would fit (Figure 5.6).

**Figure 5.6 – CAD Model of the box and its contents**

5.8 Payload

Payload is the additional weight or equipment carried by aircraft, excluding the essential components needed for flight, such as the motor, battery, and control system. For the mission, the payload is designed to weigh at least 2.13 lbs, which is 30% of the aircraft's total weight. The

payload weight was chosen to maximize score; a heavier payload is better for scoring, but too high would make it more difficult to attain a realistic thrust-to-weight. The dimensions where the payload sits are 3.25 x 3.25 x 6 in, as seen in Figure 5.8, which were selected to allow the payload to fit perfectly inside the fuselage and meet the minimum required dimension (Figure 5.8b).



(a) Payload Box



(b) Payload fitted inside the Fuse

Figure 5.7 – Payload Layout

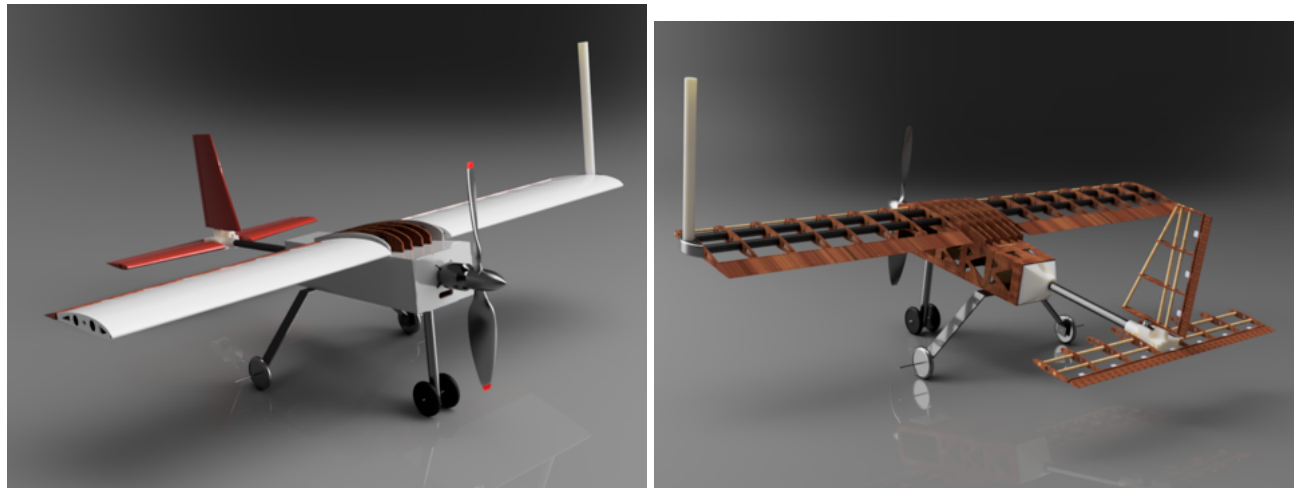
5.9 Weight and Balance

To ensure the plane's center of gravity stays in front of the center of lift, the electronics were all placed towards the front of the plane's fuselage. The electronics include the telemetry receiver, battery, ESC, and the main motor plus propeller. This allowed for the payload to be placed behind the center of lift without significantly moving the center of gravity. By using aluminum rear landing gear, the design for using a $\frac{3}{4}$ inch PVC pipe and PVC couplers for the front landing gear was to aid in balancing the weight of the back from the front landing gear. The boom-fuse connection was designed to be sturdy but structurally secured for holding the tail without any tolerances. The boom was designed to add 16 inches in length to the tail from the boom-fuse connection that will assist in creating a stabilizing moment while the plane is in flight. The rear landing wheels spacing was 16 inches and mounted 14 inches from the front wheel to ensure proper balancing on the runway and for stable landing. Dimensions in 5.3 are listed with the origin at the center of the leading edge of the aircraft main wing. X is longitudinal, Y is lateral, and Z is vertical.

Table 5.3 – Weight Balance For Each Mission

Component	Weight [lbf]	x [in.]	y [in.]	z [in.]
Mission 1 (Empty)				
Fuselage	1.850	2.000	0.000	-2.400
Rear Connector	1.02	8.00	0.0	-3.50
Tail Boom	0.250	20.40	0.0	-2.40
Front Landing Gear	0.063	-3.50	0.0	-6.0
Front Landing Gear	0.125	9.300	0.0	-6.2
Wing	1.25	4.05	0.000	0.043
Motor	0.641	-4.40	0	-3.00
H-Stabilizer	0.086	29.99	0.000	-3.052
V-Stabilizer	0.051	29.21	0.000	2.536
Battery	1.253	-3.000	0.0	-2.80
ESC and Reciever	0.063	-3.500	0.0	-2.40
Monokoting and Bolts	0.273	-3.50	0.0	-1.0
Total	6.901	4.02	0.0	-2.19
Mission 2 (With Payload)				
Payload	2.130	3.000	0	-2.500
Total with Additions	9.03	3.174	0.0	-2.427
Mission 3 (Jamming Antenna)				
Jamming Antenna and Assembly	0.273	16.200	0.000	-2.000
Counter Weight	0.273	3.500	0.000	-0.250
Total with Additions	9.577	3.249	0.0	-2.29

5.10 Final 3D Render



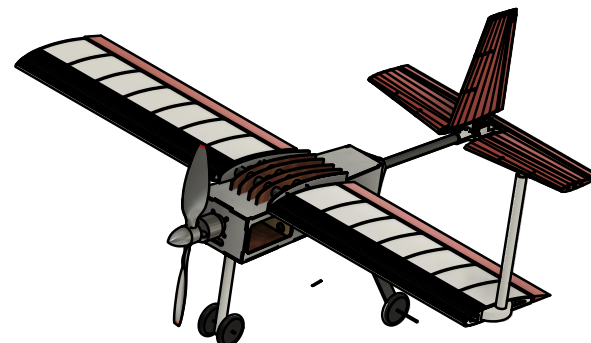
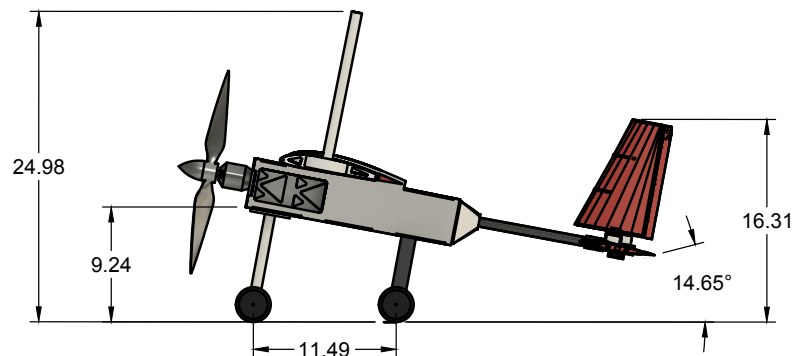
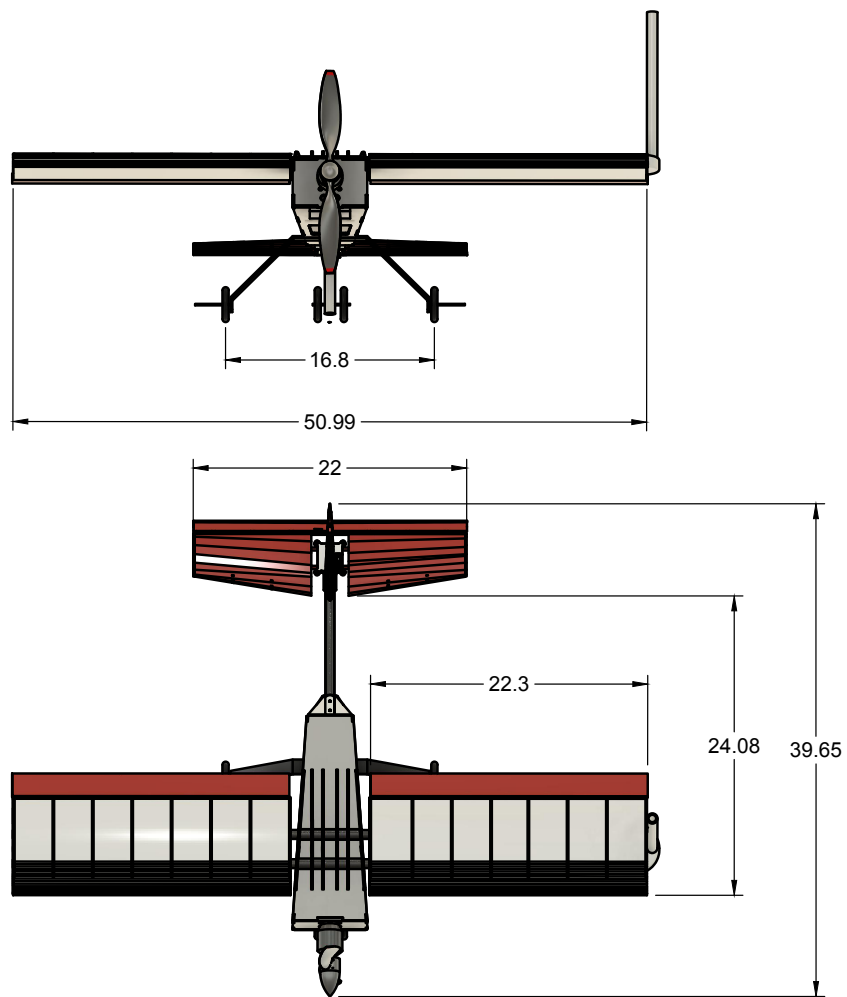
(a) Payload Dimensions

(b) Payload fitted inside the Fuse

Figure 5.8 – 3D Render Layout

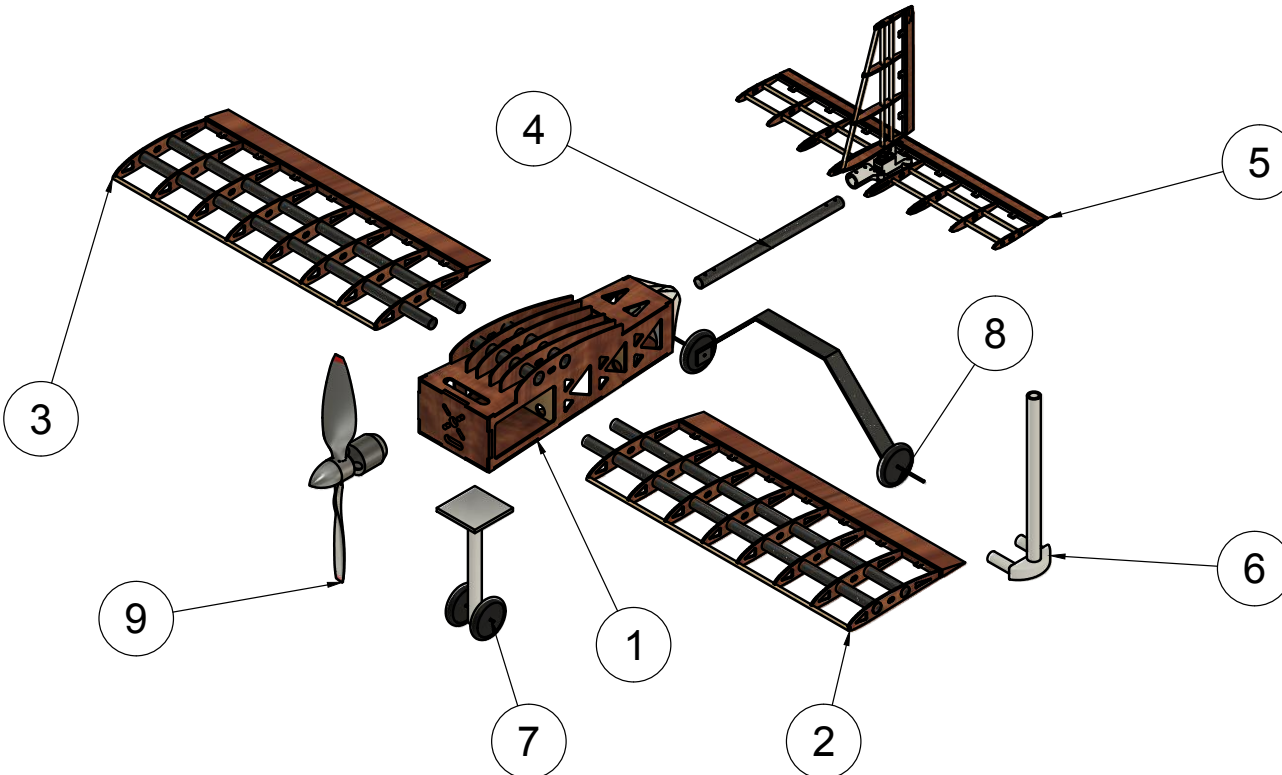
5.11 Drawing Package

A drawing Package is shown down below as follows:



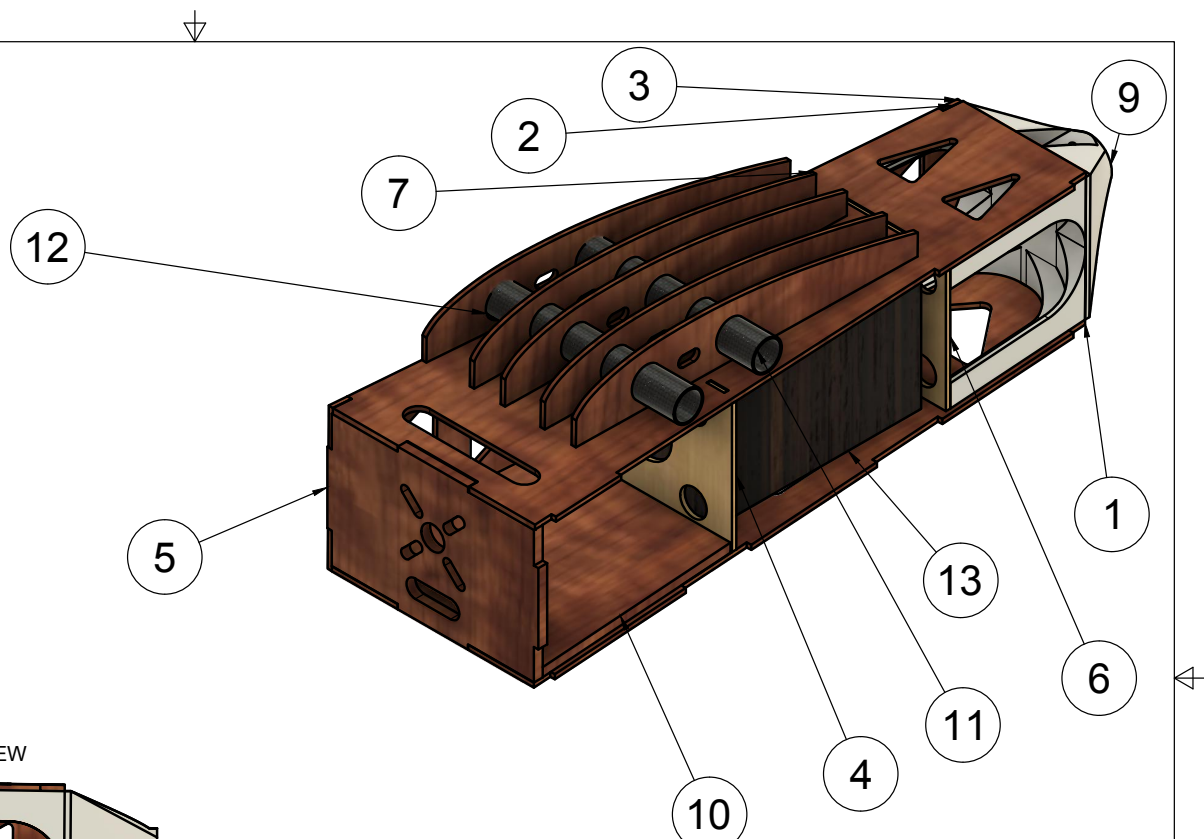
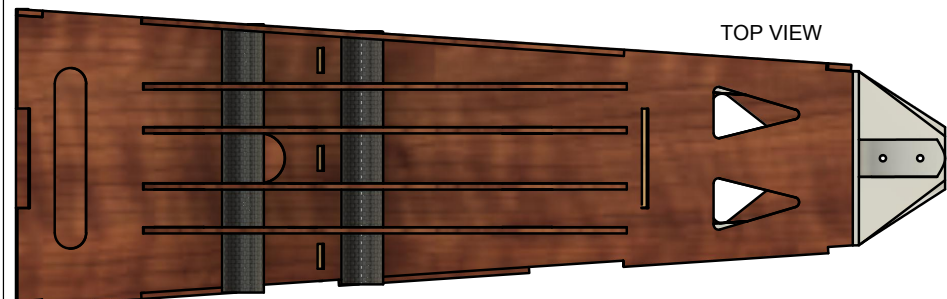
ILLINOIS TECH STUDENT BRANCH aiaa.iit.edu		PROJECT AIAA DESIGN BUILD FLY 2023		
		TITLE 3-VIEW LAYOUT GOON-HAWK 02/17/2023		REV 1
APPROVED MURAT VURAL	SIZE B	CODE 0000	DWG NO 0001	
CHECKED EYOB GHEBREIESUS				
DRAWN CHRISTOPHER FOLKER	SCALE 1:10	WEIGHT 9.38 LB	SHEET 1/4	

PARTS LIST		
ITE M	QTY	PART NUMBER
1	1	5000 - FUSELAGE
2	1	4100 - LEFT WING
3	1	4200 - RIGHT WING
4	1	2000 - BOOM
5	1	3000 - TAIL ASSEMBLY INCIDENCE
6	1	ATTENA AND COUPLER ASSEMBLY
7	1	FRONT LANDING GEAR ASSEMBLY
8	1	8100 - SHORTENED REAR GEAR
9	1	POWER60_15PROP_WNOSE

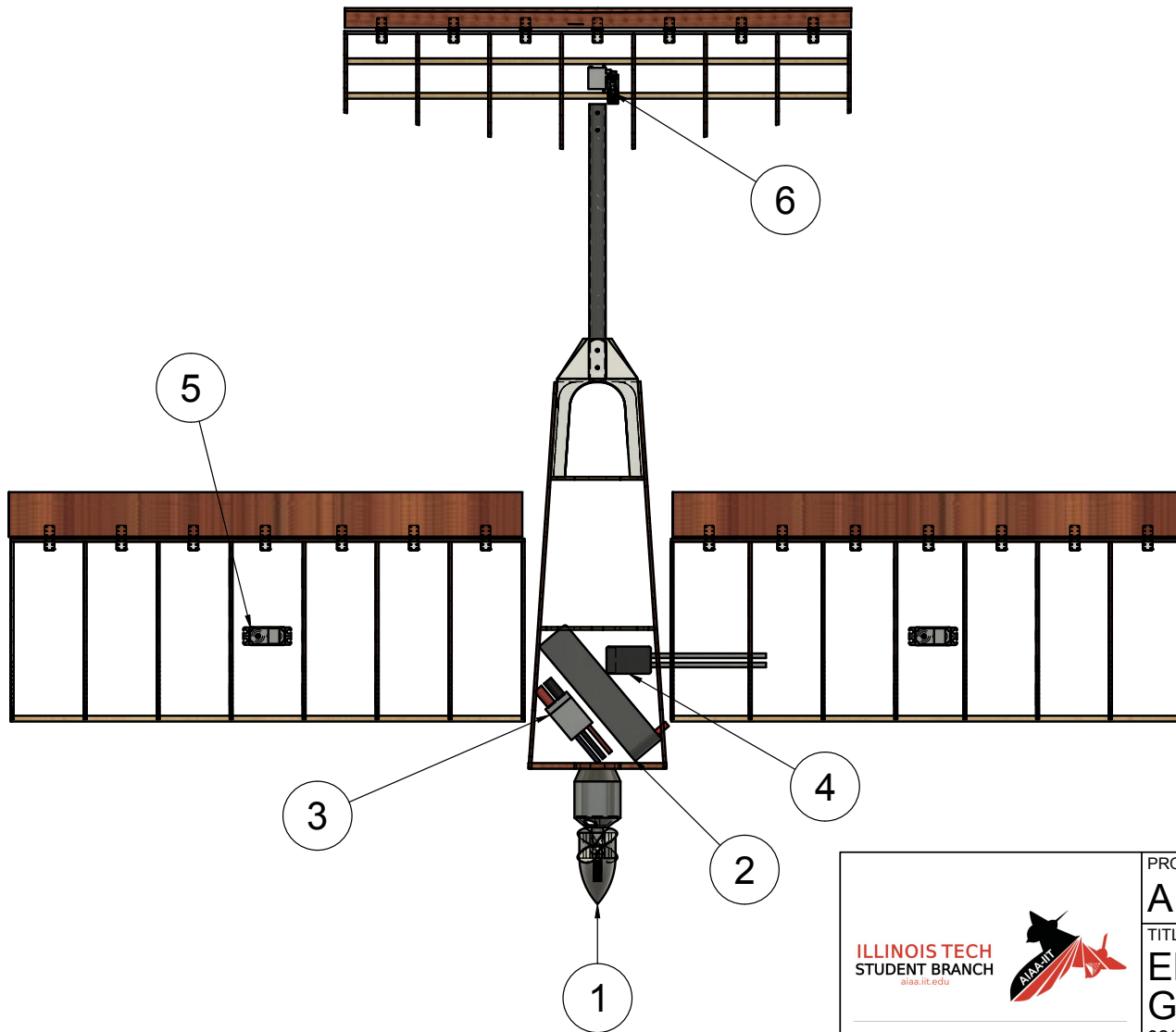


ILLINOIS TECH STUDENT BRANCH 	PROJECT		
	AIAA DESIGN BUILD FLY 2023		
TITLE			
STRUCTURAL LAYOUT GOON-HAWK			
02/17/2023			
APPROVED MURAT VURAL	SIZE B	CODE 0000	DWG NO 0002
CHECKED EYOB GHEBREIESUS			
DRAWN CHRISTOPHER FOLKER	REV 1		
SCALE 1:7.5	WEIGHT 7.21 LB	SHEET 2/4	

PARTS LIST		
ITEM	QTY	PART NUMBER
1	1	5001 - BOTTOM PLATE
2	1	5002 - SIDE PLATE
3	1	5003 - TOP PLATE
4	1	5004 - FRONT BULKHEAD
5	1	5006 - FRONT PLATE
6	1	5005 - REAR BULKHEAD
7	4	5007 - FUSE TOP RIB
9	1	5008 - TAIL CONNECTION
10	1	5004 - ELECTRONICS BAY PLATE
11	1	5009 - FUSELAGE SPAR BACK
12	1	5008 - FUSELAGE SPAR FRONT
13	1	PAYOUT



ILLINOIS TECH STUDENT BRANCH aiaa.iit.edu	PROJECT AIAA DESIGN BUILD FLY 2023		
	TITLE PAYOUT ACCOMODATION GOON-HAWK 02/17/2023		
APPROVED MURAT VURAL	SIZE	CODE	DWG NO
CHECKED EYOB GHEBREIESUS	B	0000	0003
DRAWN CHRISTOPHER FOLKER	SCALE 1:2	WEIGHT 3.27LB	SHEET 3/4



PARTS LIST		
ITEM	QTY	PART NAME
1	1	POWER60_15PROP_WNOSE V5
2	1	7400 - MAIN BATTERY V1
3	1	CASTLE 105A ESC V1
4	1	SPEKTRUM RECIEVER V1
5	2	7300 - SERVO V2
6	1	3000 - TAIL ASSEMBLY INCIDENCE V19
9	1	5000 - FUSELAGE V64
10	1	4100 - LEFT WING V18
11	1	4200 - RIGHT WING V13
12	1	2000 - BOOM V13

PROJECT AIAA DESIGN BUILD FLY 2023				
TITLE ELECTRONICS LAYOUT GOON-HAWK 02/17/2023				
APPROVED MURAT VURAL	SIZE	CODE	DWG NO	REV
CHECKED EYOB GHEBEREIESUS	B	0000	0004	
DRAWN JAMES SZEWczyk	SCALE	1:7.5	WEIGHT 2.58LB	SHEET 4/4

6 Manufacturing Plan

6.1 Manufacturing Plan

The team had three major stages in order to obtain the aircraft depicted in this report: Design, Manufacture, and Test. Adhering to the design configurations and specifications outlined in the Detailed Design section of the report, the team was able to manufacture the aircraft in a manner to optimize the flight performance and structural integrity. Weighing on the team's past experiences in manufacturing and influenced by the design of the aircraft, three main manufacturing methods were considered for components: 3D-Printing, Laser Cutting, and CNC Milling. Additionally, the team was able to finalize three materials for primary manufacturing due to the ability to procure the material, the strength and weight of the material, and the ease of manufacturing: Composites, Plywood, Balsa Wood, and High-Density Foam. Upon selecting the method and material used for manufacturing, the team was able to begin manufacturing the main subsystems of the aircraft. The main subsystems for the aircraft were the wing, fuselage, and the antenna. A summary of the processes, their strengths and weaknesses, and the ultimate selection for the aircraft are found in the following sections.

6.2 Methods Considered

6.2.1 3D-Printing

To connect the tail to the boom, a 3D printed part was used. By 3D printing, the team was able to make the connector from Acrylonitrile Butadiene Styrene (ABS), a strong material capable of withstanding forces that may try to pull pieces apart, yet also lightweight enough to not hinder flight. Polylactic acid (PLA) is a cheaper and lighter weight material used in 3D printing, which is good for pieces that do not have as much force acting upon them, such as the antenna mount.

6.2.2 Laser Cutting

To cut parts made of wood, laser cutting is the best method because of how much more precise it is compared to cutting by hand.

6.2.3 CNC Milling

CNC milling is a process by which a CAD model is loaded into a CAM software where the designer selects the order and method by which the particular model is to be cut. The most difficult part of this method is just making sure the correct instructions are given to the computer because the CNC machine does all the physical work. Although somewhat time consuming, CNC is more accurate and does not require as much assembly as a balsa wing with many laser cut parts.

6.3 Materials Considered

There are several factors in material choice, but the ones the team focused on are weight, ease of manufacturing, and durability, the most important being ease of manufacturing. Composites and wood were the two materials considered for this design.

6.3.1 Composites

Using composites for the wings rather than wood and MonoKote has many advantages. MonoKote can puncture easily and there is risk of the wooden ribs fracturing, while composite wings are more durable. Also, a composite wing can take less time to make because there are fewer parts to fuse together. It is easier to do tapered wings or elliptic wingspans because the pink foam used as a positive mold can be easily cut to any shape.

A major disadvantage to composites is the resources it requires. Once the foam is cut (which requires a CNC machine), the composite layup is done with fiberglass and epoxy. Ideally, the wing is put in a curing oven after this, but the team does not have access to one so the wing would have to air dry. While this is possible, it is not desirable, which is why composites were not selected as the final material.

Carbon fiber rods were considered for the spars and tail boom because it is lightweight yet durable. Carbon fiber rods are commercial off the shelf (COTS) and the only manufacturing required is cutting them to size and attaching, making them a good choice for the previously specified components.

6.3.2 Ply and Balsa Wood

The classic material for RC airplanes is balsa wood. Although balsa wings are more fragile and time consuming to make, they are simpler to assemble. The laser cutter accurately cuts all the pieces to size, then those pieces are put together using dowels and Cyanoacrylate adhesive (CA), then sealing irons are used to press on the MonoKote that encases it.

For the fuselage, a thin plywood is used because something stronger than balsa is needed to support the motor propeller and hold together all the other parts of the aircraft. It is better to use wood for the fuselage because spaces can be left more easily to mount parts, connect them, and store electronics. The same method of laser cutting and fusing together with glue, then sealing with MonoKote is used.

6.4 Subsystem Manufacturing

The subsystems of the aircraft are the two sets of wings, fuselage, antenna, tail, and landing gear.

6.4.1 Wing Set 1

The creation of Wing Set 1 can be broken down into two main processes, fabrication and assembly. More time was devoted to the fabrication process to ensure that the components of the wing were cut and sanded to the utmost precision to make the assembly process run

smoothly.

To start off the fabrication process, two carbon fiber dowels were measured and cut to size using a band saw. These dowels acted as the wing's main spars and had holes drilled through them on one end where bolts would later secure them to the fuselage. The wooden spar running down the leading edge was also cut to length using a fine handsaw. After cutting the main spars, Balsa wood ribs were cut out using a laser cutter and were test fitted. The ribs were also sanded whenever necessary to ensure they slid smoothly along the spars. Next, the flaperons were cut out of balsa wood planks using a table saw with an angle blade. The flaperons were then taken to a sander, where any extra material left by the table saw was removed. Lastly, the balsa wood backing plate and $\frac{1}{32}$ in. balsa sheet were measured and cut to size.



Figure 6.1 – Wing Manufacturing

With all the components cut out, the wing underwent a test-fitting phase. Both wing sections were temporarily assembled, and any additional sanding and adjustments were made to ensure the components fit perfectly. Using CA, the balsa wood ribs were evenly spaced and glued to the carbon fiber spars, see Figure (6.1). The leading edge spar and backing plate were done in a likewise fashion. With the wing structure assembled and fastened, the balsa wood sheet was carefully laid on top of the wing section, starting at the leading edge and following the ribs' profile to around the quarter chord point. After the CA was given time to cure, MonoKote strips were cut and then adhered to the wing's surface using a heat gun and heating iron. Finally, with the MonoKote finished, small corresponding incisions were made in the backing plate and flaperons. Small plastic hinges were slipped and glued into these small cuts to connect the flaperons to the rest of the wing.

6.4.2 Wing Set 2

The same process as Wing Set 1 was used in order to create Wing Set 2. Both the wing sets shall be marked accordingly so they can be easily identified at the competition. For Wing Set 1, the wings will be labeled as Left Wing - 1 and Right Wing - 1. Similarly, Wing set 2 will be

labeled as Left Wing - 2 and Right Wing - 2.

6.4.3 Fuse

The fuselage is made out of plywood sections laser cut from CAD files. The sections are then ensured to fit perfectly after which, using the CA, the motor plate, two bulkheads and the four top-mounted ribs are secured together. After the CA was given time to cure, the carbon-fiber spars were fitted within the ribs, see Figure 6.2. The carbon-fiber spars were glued using CA and given time to cure. Next, MonoKote strips were cut and they are adhered to the fuselage using a heating iron and heat gun. The tail connector is attached to the end of the fuselage. The tail connector is 3D-printed using ABS with a 40% infill to be able to withstand the forces it will encounter. After the MonoKoting, the tail connector was attached using CA and was given time to cure.



Figure 6.2 – Fuse Manufacturing

6.4.4 Antenna

The antenna is made of $\frac{1}{2}$ inch Schedule 40 PVC and is 15 inches long. The PVC was cut to size using a saw, and mounted on to the wing with a 3D printed piece made of PLA. On the wing without the antenna, a counterweight piece also 3D printed from PLA was attached. The counterweight piece is slightly heavier because it needs to offset the weight of the antenna and mount on the other wing.

6.4.5 Tail

The rib sections for the elevator and the rudder were laser cut from CAD files of the design. The spar dowels were then cut to length and the elevator and rudder were mocked up before CA was applied. Once the elevator and rudder were set up and glued in place, MonoKote was applied over all control surfaces. The elevator and rudder flaps were cut from balsa wood stock with the appropriate angles and were attached using RC aircraft flap hinges. The clam-shell mounting pieces were 3D printed using ABS plastic with 40% infill. Finally, the carbon fiber boom section was cut to length and mounting holes were drilled through it. With all the

pieces fabricated, the tail could be fully assembled. The vertical and horizontal stabilizers can be seen in Figures 6.3a and 6.3.



(a) Manufactured Vertical Stabilizer



(b) Manufactured Horizontal Stabilizer

Figure 6.3 – Manufactured Horizontal Stabilizer

6.5 Landing Gear

For the landing gear, PVC pipe was used for the front and metal for the back. A $\frac{1}{16}$ inch hole was drilled through one end of the PVC pipe perpendicular to the surface so a steel axle shaft can be threaded into. The wheel was slipped onto the axle shaft and locked into place while still being able to rotate easily by using a shaft lock collar.

6.5.1 Box Manufacturing

The purpose of the box is to transport all of the airplane parts and what is needed to assemble them. The box is made out of $\frac{1}{4}$ inch medium density fiber board (MDF) as seen in Figure 6.4, and was fitted together through the use of corner braces, screws, and wood glue. Holes were drilled in two sides to use as handles, latches were added to the lid to secure the lid, and a hinge was added to keep the lid attached. Figure 6.4b also shows that all the plane components fit inside the shipping box.



(a) Shipping Box Manufactured

(b) Shipping Box with all Plane components Inside

Figure 6.4 – Shipping Box Manufacturing

6.6 Manufacturing Milestone Chart

The team's manufacturing plan and milestone is displayed in [6.5](#). The team will be utilizing a, laser cutter, and 3D printer to manufacture components. The aircraft will be constructed using balsa and plywood with a MonoKote skin. The team will manufacture two proof of flight aircraft to determine the optimum aircraft system design and configuration. The Chief Engineer assists the structures sub-team in designing components based off of data provided by the sub-team leads. Design drawings are shared with all team members for manufacturing and assembly.

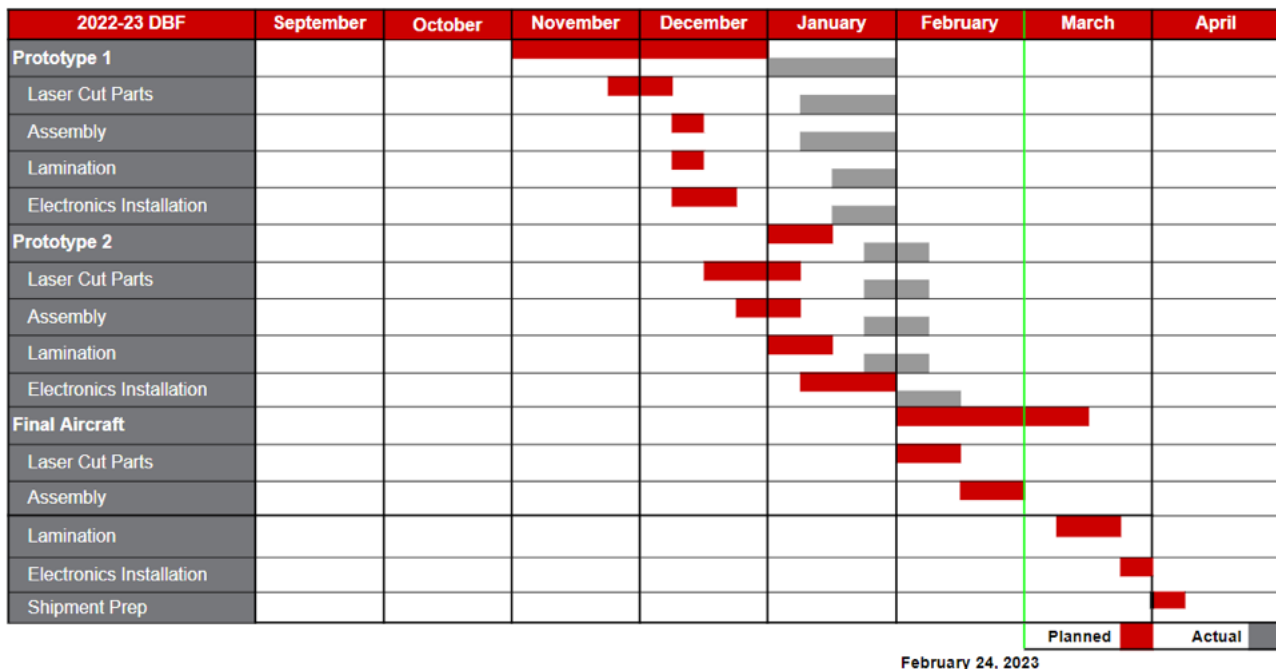


Figure 6.5 – Manufacturing Milestone Chart

7 Testing Plan

Theoretical predictions of aircraft performance were tested to assess their validity. In addition, tests were performed to find the ideal combination of the subsystems: aerodynamics, propulsion, and structures. Subsystem relationships were tested for each mission to determine maximum efficiency of overall aircraft performance.

7.1 Testing Milestone Chart

There are three main subsystem categories that need to be tested: aerodynamics, propulsion, and structures. After this a flight test is conducted to confirm the plane's over all performance. The testing schedule and milestone are broken down in Figure 7.1 showing the planned (red), and actual (gray) testing schedules.

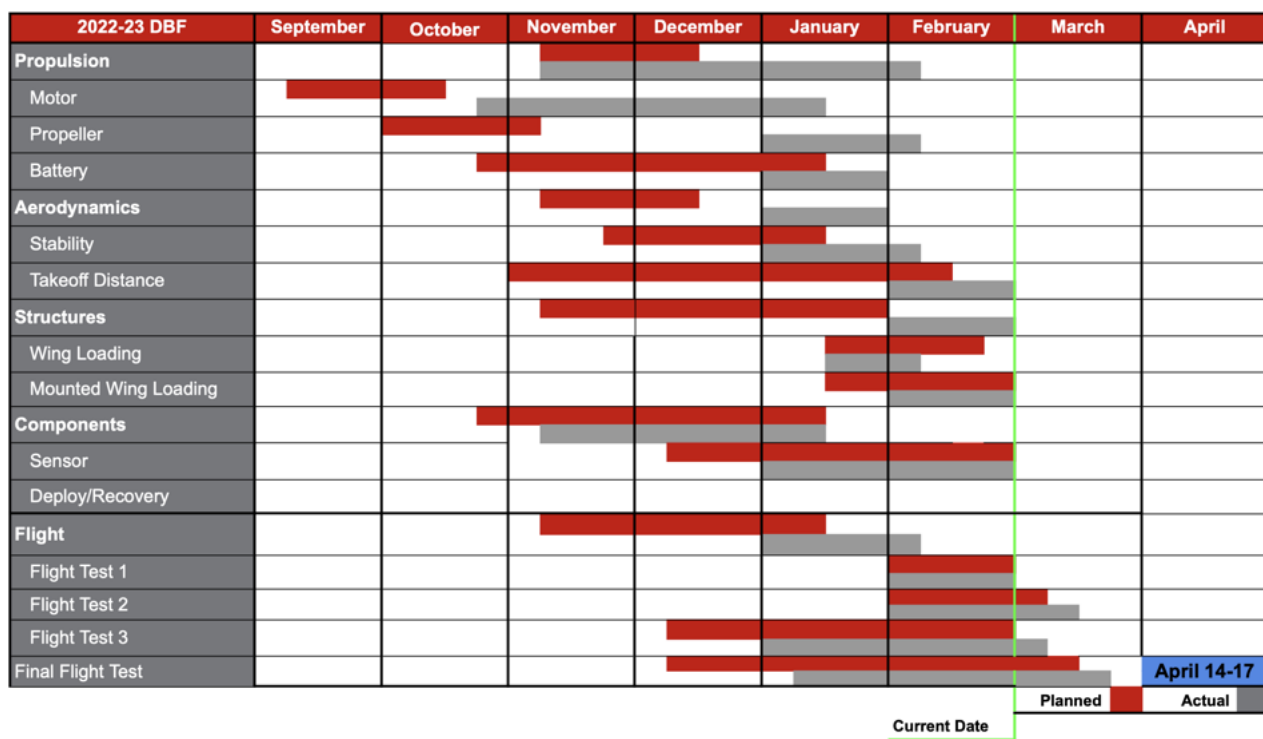


Figure 7.1 – Testing Milestone Chart

7.2 Structural Test

In order to determine if our aircraft would withstand all forces experienced during flight, our team conducted the following structural tests. The first structural test that the team performed was a Finite Element Analysis (FEA) of the wing. This FEA would be used as a proof for our wing-tip test to ensure our design would allow for the aircraft to withstand all aerodynamic forces. In order to do this analysis, the team applied the maximum load of the aircraft at the root chord of the wingspan. Upon passing the FEA, the team would then conduct a wing tip test. The wing tip test was conducted by configuring the aircraft with an empty load and then a thirty percent of maximum load. Refer to Figure 8.1 for the FEA of the wingspan and 8.4 for the Wing Tip Test.

7.3 Motor Test

The purpose of these tests is to evaluate the static thrust, current draw, expected flight time, and motor temperature of the motors in consideration for the aircraft. By using on-board ESC data collection, motors were run on a test stand to collect wattage, thrust, temperature, motor RPM, and amperage for a variety of motor and propeller combinations. These data points could then be evaluated after the test to generate throttle curves, flight time estimates, as well as verify the predictions of the conceptual design eCalc models.

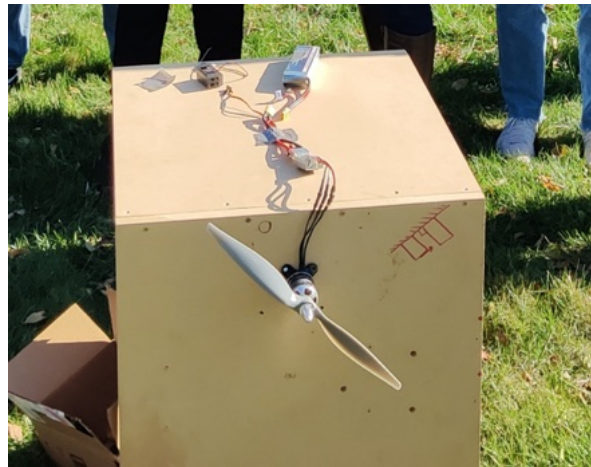


Figure 7.2 – Motor Test Configuration

Each of the configurations tested were mounted and secured to a test stand. The ESC, receiver, and battery were then wired to the motor and secured. For each test, a 5S 5000 maH LiPo battery was charged to 4.2 volts prior to testing, and the same 100A Castle ESC used for all configurations. All tests were conducted outside, and in a safe environment. The setup was not shielded from wind to provide perturbations during tests to better simulate flight conditions, and temperature was not considered to be a significant factor as tests were of short duration (less than 10 minutes) and all batteries were kept at 72 degrees Fahrenheit until immediately before testing. Lithium battery performance is known to degrade with high and low temperatures, but high temperature environments necessary to better simulate the location of the competition were unavailable to the team.

7.4 Wing Tip Test

A wing tip test will be conducted by attaching the aircraft to a ground-test fixture, which would fix the aircraft in a manner that a point load would be applied at the end of each side of the span of the wing. This point load at each end of the span would be equal to one half of the aircraft weight whenever it is empty and at thirty percent of the maximum weight. This will allow the team to demonstrate that the aircraft can withstand varying aerodynamic forces throughout flight prior to a test flight. Furthermore, this test will test the teams manufacturing capabilities by comparing the FEA results to the actual wing tip test results. Refer to Figure



8.4 for the Wing Tip Test being conducted by the team.

7.5 Flight Test

After all components tests are completed, the aircraft will be flight tested multiple times before the competition. In-flight data will be collected using the electronic speed controller to record the data points. The proof of concept test flight will validate the aircraft configuration and wing sizing. Following each prototype cycle, results will be evaluated and improvements implemented into future iterations. The final flight test will be conducted with the competition aircraft and will fully simulate all missions to ensure expected performance goals are met.

7.6 Flight Test Check List

The team followed a pre-flight and flight checklist shown in 7.1, and 7.2. This was done to ensure proper data collection and efficiency. Each category allowed for the specific tasks regarding aircraft inspection and maintenance.

Table 7.1 – Preflight checklist

Component	Task
Fuselage (Internal)	<input type="checkbox"/> Secure and Connect the Fully Charged Battery <input type="checkbox"/> Receiver has All Connections Plugged in and Secured <input type="checkbox"/> Verify CG <input type="checkbox"/> Load Electronics Package (if applicable)
Fuselage (External)	<input type="checkbox"/> Close and Fasten <input type="checkbox"/> Secure Nuts and Bolts <input type="checkbox"/> Check all control surfaces with receiver
Pilot Checks	<input type="checkbox"/> Motor Run Up <input type="checkbox"/> Go/No-Go

**Table 7.2 – Flight checklist**

Component	Task
Before Flight	<input type="checkbox"/> Propeller Secure <input type="checkbox"/> Fasteners Secured <input type="checkbox"/> Connections Secured <input type="checkbox"/> Battery Charged/Secured <input type="checkbox"/> Free/Connect Control Surfaces <input type="checkbox"/> Plug in Receiver Pack <input type="checkbox"/> Receiver Pack Connected <input type="checkbox"/> Payload Secure <input type="checkbox"/> Antenna Fully Deployed
During Flight	<input type="checkbox"/> Payload Check <input type="checkbox"/> Counter Weight
After Test	<input type="checkbox"/> Throttle Idle <input type="checkbox"/> Battery Disconnected

8 Performance Results

8.1 Structural Endurance Results

The Finite Element Analysis was simulated and solved for as described in Section 7.1 using a weight of 9 pound-force acting at the root chord of the span. Upon completing the simulation the team was able to obtain the results shown in Figures 8.1 and 8.2. The figures show that the design of the wing was adequate for the mission as the FEA showed little stress and strain taking place along the structure. This means that the aircraft will comfortably fly in the missions outlined in this years rules.

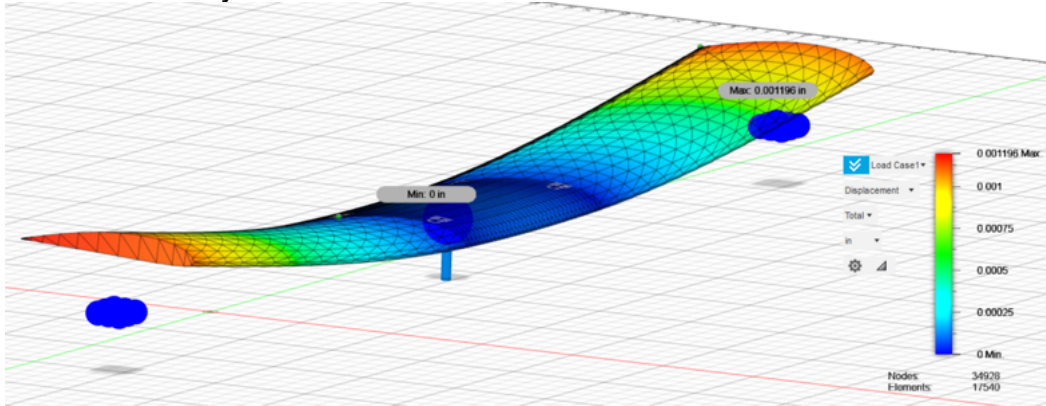


Figure 8.1 – Wing Tip Displacement Analysis

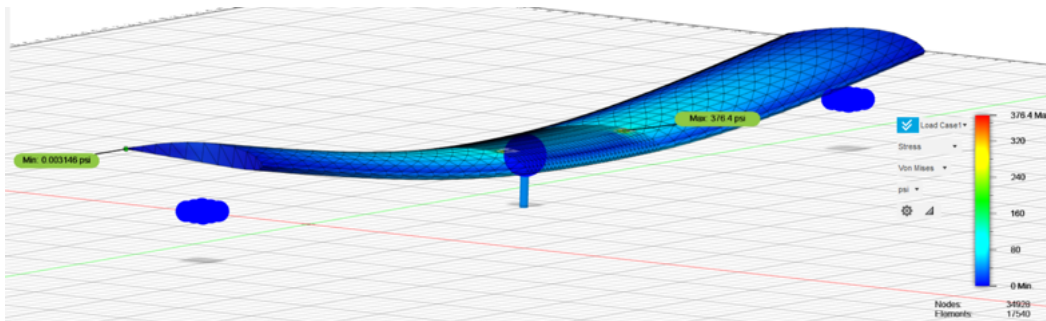


Figure 8.2 – Wing Tip Stress Analysis

8.2 Propulsion Results

Testing was done with the Turnigy Aerodrive SK3-4025 and E-flite Power 60B motors to determine thrust and efficiency differences between the two. Both motors were tested with the same 16 x 8 APC Electric propeller on the same day. Voltage sag was considered negligible through the duration of the test. Each motor was run for at least 20 seconds at throttle from 55% to 100% in increments of ten percent throttle. This data in Figure 8.3 was then recorded from the Castle Link program.

This data was then read from the ESC in CSV files, and used to determine the results shown

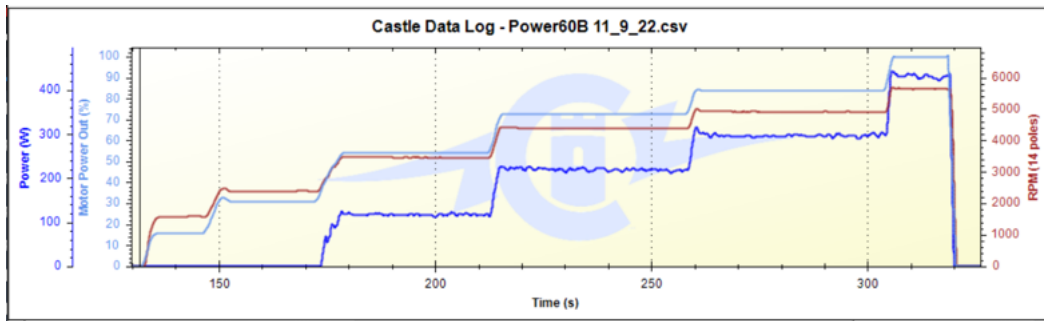


Figure 8.3 – Castle Link Graph of the Power 60B

in 8.1 below. The thrust targeted for cruise was 6.8 pounds force. Flight time was estimated using 80% battery capacity and the averaged wattage at the cruise thrust level.

Table 8.1 – Motor Test Results

Parameters	Power 60	Aerodrive Sk3
Maximum Thrust (lbf)	8.66	7.98
Peak Power Draw (Watts)	585	573
Cruise Thrust Throttle Percent	85	90
Cruise Throttle Est. Flight Time (minutes)	11.1	10.0
Peak Amperage	32.6	31.7
Weight (lb)	1.11	0.787

From these tests, the Power 60 is the preferred motor for flight tests, with a greater static thrust and greater cruise time. However, the Power 60 is significantly heavier than the Aerodrive. For this reason, the Aerodrive may be used as a backup alternative, in the event structural or weight concerns affect the craft. Ballast would be required to offset the weight difference, and could be mounted in the electronics bay.

8.3 Wing Tip Test Result

The team was able to carry out the wing tip test per the manner described in Section 7. The team lifted the empty aircraft by placing a finger at the end of each side of the span. Furthermore, the team was able to carry out the test for the 30% minimum load by placing the ends of the span on stools. That is 2.2lbf of load on the fuse. This load is then increased slowly until the wing reached its maximum tension of 4.7lbf. Both tests were deemed successful as the aircraft was able to sustain itself from the point loads placed on each edge of the span. Refer to Figure 8.4 for the successful Wing Tip Tests being conducted by the team.

8.4 Flight Test Result

A flight test of the first prototype competition aircraft was conducted to test its performance and handling capabilities. The primary purpose of this flight test was to confirm critical performance values, including the aircraft's ability to take off within a maximum allowable distance of 60 feet. The value in Table 8.2 was obtained as a result of the first flight test.



(a) Empty Weight Wing Tip Test



(b) Wing Tip Test with 30% Payload (2.20lb) Weight.



(c) Wing Tip Test with Jamming Antenna .

Figure 8.4 – Wing Tip Test**Table 8.2 – Flight Test Results**

Parameters	Results	Required Parameter
Temp	44°F	-
Gust Wind	33mph	-
Take off Distance	45ft	≤ 60ft
Flight Speed	24mph	-

During the takeoff, the aircraft's performance was assessed by measuring the maximum distance it covered (45 ft) before becoming airborne as seen in Figure 8.5. No major complications arose during the takeoff. However, after airborne some adverse signs were observed during flight. The team assessed the results of the flight test against the predicted performance, and will modify some components of the plane improve its aerodynamics efficiency. More flight testing will be conducted before the the official competition that correspond to each mission profile.



(a) Taxi



(b) Take-off.



(c) Fly-by

Figure 8.5 – Flight Test

8.5 Comparison of Prediction vs. Actual

Based on aerodynamic, stability, and propulsion calculations, the aircraft was predicted to fly well up to speeds of 43 miles per hour and an angle of attack of 11° before stalling. In actuality, the plane did not meet the speed target, only reaching 38 mph, as speed was estimated using a curve fit method. The stall speed was correctly predicted at 24 mph, and the angle of attack



of stall was also 11 degrees in testing. There was a significant adverse yaw effect experienced during roll, as caused by the large flaperon surfaces. In addition, there was low roll stability during flight tests. These two issues will hopefully be diminished by an increase in vertical tail size. Additionally, the usage of partial flap deflection should minimize the effects during takeoff and landing by constraining the control surface deflection and increasing lift. A covering will also be fitted to the center wing section for delaying stall and increasing lift.

References

- [1] "2022-23 Design, Build, Fly Rules", AIAA [online],
- [2] Hepperle, M., <https://www.mh-aerotools.de/airfoils/index.htm>
- [3] Loftin Jr., L. K., "Appendix C", *Quest for Performance: The Evolution of Modern Aircraft*, NASA Scientific and Technical Information Branch, Washington D.C., 1985. <https://www.hq.nasa.gov/pao/History/SP-468/cover.htm>
- [4] Prasuhn, A. L., *Fundamentals of Fluid Mechanics*, Prentice-Hall, 1980.
- [5] Raymer, D. P., *Aircraft Design: A Conceptual Approach*, 6th ed., AIAA, 2018.
- [6] White, F., *Fluid Mechanics*, McGraw-Hill, New York, 2011, pp. 484-485.